SLIDING MODE CONTROL OF A TWO DEGREES OF FREEDOM HELICOPTER SYSTEM

by

Hilmi Artun Oyman

B.S., in Electrical Engineering, Yıldız Technical University, 2008

Submitted to the Institute for Graduate Studies in
Science and Engineering in partial fulfillment of
the requirements for the degree of
Master of Science

Graduate Program in Systems and Control Engineering
Boğaziçi University
2012

ACKNOWLEDGEMENTS

First of all, I would like to thank to all the people who supported and encouraged me during my MS degree.

I'm at a loss for words to express my gratitude to my thesis supervisor, Assoc. Prof. Yağmur Denizhan, for her guidance, endless support and patience in preparation of this study. Her working discipline greatly motivated me.

I would like to thank Prof. Eşref Eşkinat and Prof. Işıl Bozma for their attendance to my thesis committee.

I would also like to thank dynamical systems laboratory assistants Deniz Seviş, Kamil Şenel and Gökhan Habiboğlu for their helpfulness. Many thanks to mechatronics laboratory researchers, Çisel Aras, Yeşim Öniz and Telman Raoofi, for sharing their knowledge and experiences with me. They were always patiance and willing to answer my pop-up questions.

Special thanks to my best friend Delalcan Kılıç for spending his time to correct my writing mistakes. His strong encouragement and advices were the driving force of my efforts.

Son olarak, yüksek lisans çalışmam boyunca beni hep destekleyen ve yanımda olan aileme sonsuz teşekkürlerimi sunarım.

This thesis has been supported by Bogazici University Scientific Research Project Grant No: 5683P

ABSTRACT

SLIDING MODE CONTROL OF A TWO DEGREES OF FREEDOM HELICOPTER SYSTEM

In this thesis, one of the robust control methodologies, namely Sliding Mode Control (SMC) is applied to Quanser's Two Degrees of Freedom Helicopter System (2-DOF-HS) and the performance of this approach is compared with the performances of other control methods such as Full State Feedback Control (FSFC) via Linear Quadratic Regulator (LQR) and Feedback Linearization (FL) with Pole Placement. Firstly, the mathematical model given by the manufacturer is investigated. Various parameters such as torque and friction constants are calibrated by trial and error. The mass of the system is assumed to be uncertain yet is bounded between the nominal mass and the mass with the maximum additional load. The nonlinear Multi-Input-Multi-Output (MIMO) sliding mode controller is designed in such a way that the uncertainties are taken into consideration. Control input is interpolated in a constant boundary layer to reduce the chattering problem. Finally, SMC is observed to give better results than the other approaches.

ÖZET

KAYAN KİPLİ DENETİM YÖNTEMİ'NİN İKİ SERBESTLİK DERECELİ HELİKOPTER SİSTEMİNE UYGULANMASI

Bu tezde, deneysel çalışmalar için Quanser firması tarafından üretilen 2 serbestlik dereceli helikopter seti, gürbüz bir denetim yöntemi olan Kayan Kipli Denetim (KKD) yaklaşımıyla denetlenmiş, bu yöntemle elde edilen sonuçlar, Tam Durum Geribeslemeli Denetim ve Kutup Atama ile Geribeslemeli Doğrusallaştırma yöntemlerinin sonuçlarıyla karşılaştırılmıştır. Öncelikle üretici firmanın verdiği matematiksel model detaylı bir şekilde ele alınmış, sistemin tork ve sürtünme katsayılarının kalibrasyonu deneme-yanılma yöntemiyle yapılmıştır. KKD yönteminde, helikopter sisteminin ağırlığı, alabileceği maksimum yük ile yüksüz olduğu durum arasında değişken kabul edilmiştir. Sistem belirsizlikleri hesaba katıldıktan sonra çok-girdili-çok-çıktılı doğrusal olmayan Kayan Kipli Denetleyici tasarlanmıştır. Çatırtı problemi, Kayan Yüzey etrafında ince bir katman tanımlanarak azaltılmıştır. Son olarak, KKD yaklaşımının belirtilen diğer yaklaşımlardan daha iyi sonuç verdiği görülmüştür.

TABLE OF CONTENTS

LIST OF FIGURES

LIST OF TABLES

LIST OF SYMBOLS

$B_{p/y}$	Viscous friction constant around the pitch/yaw axis
g	Gravitational acceleration
$J_{p/y}$	Total moment of inertia about the pitch/yaw axis
K_{pp}	Torque constant produced by the main propeller acting on the pitch axis
K_{py}	Torque constant produced by the main propeller acting on the pitch axis
K_{yp}	Torque constant produced by the tail propeller acting on the yaw axis
K_{yy}	Torque constant produced by the tail propeller acting on the yaw axis
L	Lagrangian
l_{cm}	Distance between the center of mass of the helicopter system and the pivot
m_{heli}	Total moving mass of the system
α	Yaw angle of the system
θ	Pitch angle of the system

LIST OF ACRONYMS/ABBREVIATIONS

Q-2-DOF-HS	Quanser's Two Degrees of Freedom Helicopter System
FSFC	Full State Feedback Control
FL	Feedback Linearization
SMC	Sliding Mode Control
LQR	Linear Quadratic Regulator
MIMO	Multi-Input-Multi-Output

1. INTRODUCTION

Control theory which has been studied as an interdisiplinary branch of engineering and mathematics can be classified into two major categories, Classical Control theory and Modern Control Theory. Classical Control Theory which is based on frequency-response and root-locus methods was the first subject for the scientists because it only deals with basic systems stated as Single-Input-Single-Output systems. Afterwards, more complicated Multi-Input-Multi-Output (MIMO) systems have been investigated under the Modern Control Theory. MIMO systems can be considered as a promising research area because the improvements in computers made time-domain analysis of such complex systems possible. A simple but typical example of such systems is Quanser's Two Degrees of Freedom Helicopter System (Q-2-DOF-HS) [1] which behaves like a simplified helicopter. Since its dynamics are nonlinear and unstable, helicopter's flight control is a difficult benchmark problem in control engineering. Hence, in this thesis, this specific problem is studied on Quanser's experimental set. Initially, equations of motion of the system which are crucial for both simulation and experiments are derived by Lagrangian Method. Then, control approaches like Full State Feedback Control (FSFC) via Linear Quadratic Regulator (LQR), Feedback Linearization (FL) with Pole Placement and Sliding Mode Control (SMC) applied to Q-2-DOF-HS and their performances are invastigated.

Sliding Surface was first researched under the subject of Variable Structure Control at The Soviet Union in 1950's. A prominent property of this approach is its ability to design robust systems. SMC provides satisfactory results for the systems which have parametric uncertainties, modeling inaccuracies and are influenced by external disturbances. On the other hand, this approach has some typical drawbacks such as deterioration of actuators because of chattering. However, this problem can be handled by continous approximation of switching control law [2].

Since the mathematical model of the system has some uncertain parameters, we need Robust Control. SMC, which is a class of Robust Control, is investigated and applied to the helicopter system. On the other hand, there are various publications in the literature presenting applications of different control approaches on different helicopter systems.

Predictive Control which is easy to understand and has the ability to handle constraints is an advanced method of process control. Dutka *et al.* [3] used Humusoft's helicopter model for the tracking problem. Another control methodology which is applied to a helicopter model by M.Lopez *et al.* [4] is Feedback Linerization. The goal of the approach is to generate linear dynamics of a system from the nonlinear dynamics at hand using exact state transformations. Linear Quadratic Gaussian or so called H_2 Optimal Control was developed especially for aerospace applications around 1960's. It is a very systematic controller design method for high order and MIMO systems. S. M. Ahmad [5] proposed Optimal Control for Feedback Instrument's Twin Rotor MIMO System. Fuzzy Logic which had profound effect on the control theory emerged as a result of the 1965 proposal of Fuzzy Set Theory by Lotfi Askar-Zadeh. This approach has a critical property which translates human operator's experiences to the computer especially for MIMO systems. Gwo Ruey *et al.* [6] implemented Fuzzy Control to Q-2-DOF-HS. Juhng-Perng Su *et al.* [7], Gwo-R.Y *et al.* [8] and Q. Ahmed *et al.* [9] implemented SMC to different helicopter models. In this thesis, the sliding mode controller is designed according to the nonlinear mathematical model of the helicopter system which has not been investigated.

The organization of the thesis is as follows: In Chapter 2, Q-2-DOF-HS is introduced and its working principle is explained. In addition, mathematical model of the system is derived by Lagrange's Method. Theoretical background of the control approaches is given in the third chapter. In Chapter 4, control methodologies are applied to the helicopter system. In Chapter 5, the results of the simulations and experiments are investigated. Controllers are compared with each other on basis of performance criteria, i.e. overshoot, steady-state error, etc. The final discussions and the future works of this study are proposed in Conclusion part.

2. 2-DOF HELICOPTER SYSTEM AND ITS MODEL

Quanser's 2-DOF Helicopter System is a simplified experimental setup for invastigating some part of the helicopter dynamics. This model has a body on which two propellers are driven by two different dc motors just like the real helicopter; however, its body mounted on a fixed base as shown in Figure 2.1 [1]. Physical components of the experimental setup are given in Appendix A.

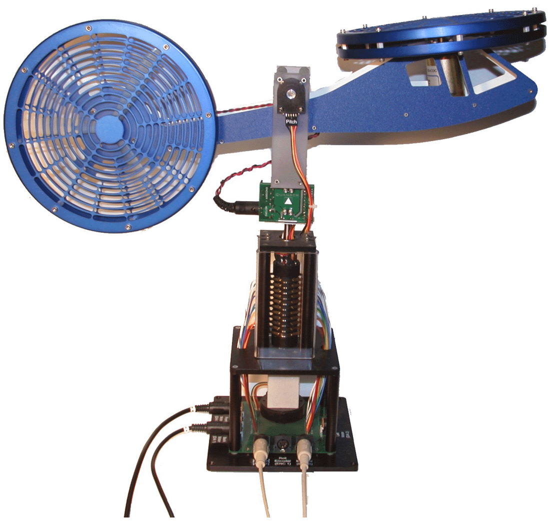

Figure 2.1. Overview of Quanser's 2-DOF Helicopter System.

The front propeller causes a rotation around the pitch axis, whereas the tail propeller rotates the body around yaw axis and generates antitorque to keep the body in balance. The pitch/yaw angle ,which is denoted by θ/α, increases positively in the counter-clockwise/clockwise direction as seen in Figure 2.2 [1]. Since these angles can be measured by the encoders for feedback, they are chosen as state variables.

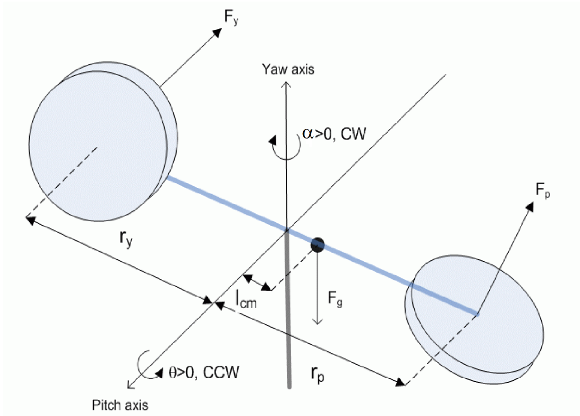

Figure 2.2. Free-Body Diagram of the helicopter system.

Now, we need to find the dynamics of the system in terms of the state variables.

2.1. Mathematical Modeling by Lagrange's Method

Lagrange's Method, which is a result of the application of Hamilton's Principle, is based on generalized coordinates and the energy of a system to express the dynamics of the system in terms of mathematical equations.

The independent coordinates used to describe the motion of a system are called generalized coordinates. The number of independent generalized coordinates are called the degrees of freedom of the system.

General form of the Lagrange's equation is stated as follows [10].

$$\frac{d}{dt}\left(\frac{\partial L}{\partial \dot{q}_k}\right) - \left(\frac{\partial L}{\partial q_k}\right) = Q_{knc} \qquad k = 1, 2, \ldots, n \tag{2.1}$$

where L is the Lagrangian, q is the generalized coordinate, $\dot{q}$ is the generalized velocity, Q is the generalized nonconservative force associated with generalized coordinate and

n is the number of degrees of freedom of the system. Lagrangian is expressed as

$$L = T - V \tag{2.2}$$

where T is the total kinetic energy of the system and V is the total potential energy of the system.

2.2. Application of Lagrange's Method to the 2-DOF Helicopter System

There are two basic approaches to derive the equations of motions for a system, namely "Newton's Method" and "Lagrange's Method". A. Rahideh [11], compared these two methods on an experimental set called Twin Rotor Multi-Input-Multi-Output System which is very similar to our system. He found that the performance of the latter method is slightly better than that of the former one. Therefore, in this thesis, Lagrange's Method is used for the derivation of the equations of motions.

Since helicopter system rotates about two independent axes, namely pitch and yaw, it has two degrees of freedom. Then, pitch and yaw angles can be selected as generalized coordinates. After changing the notation as $q_1 = \theta$, $q_2 = \alpha$, Lagrange's equations become

$$\frac{d}{dt}\left(\frac{\partial L}{\partial \dot{\theta}}\right) - \left(\frac{\partial L}{\partial \theta}\right) = Q_p \tag{2.3}$$

$$\frac{d}{dt}\left(\frac{\partial L}{\partial \dot{\alpha}}\right) - \left(\frac{\partial L}{\partial \alpha}\right) = Q_y \tag{2.4}$$

The total potential energy due to the vertical movement of the center of mass of the helicopter is

$$V = m_{heli}\, g\, l_{cm}\, sin(\theta) \tag{2.5}$$

where g is gravitational acceleration, l_{cm} is the distance between the center of mass and the pivot point. The total kinetic energy of the system due to the translation and rotation is as follows

$$T = T_p + T_y + T_t \tag{2.6}$$

where T_p is the rotational kinetic energy around pitch axis, T_y is the rotational kinetic energy around yaw axis and T_t is the translational kinetic energy. These kinetic energies are expressed as

$$T_p = \frac{1}{2} J_p \left(\dot{\theta}\right)^2 \tag{2.7}$$

where J_p is total moment of inertia about pitch axis.

$$T_y = \frac{1}{2} J_y \left(\dot{\alpha}\right)^2 \tag{2.8}$$

where J_y is total moment of inertia about yaw axis.

$$T_t = \frac{1}{2} m_{heli} \left(\dot{r}_{cm}\right)^2 \tag{2.9}$$

where m_{heli} is total mass of moving part of the helicopter system and $\dot{r}$ is generalized velocity of center of mass. In order to obtain $\dot{r}$, we need to find generalized Cartesian coordinates of center of mass.

Since the distance between the pivot and the center of mass points is l_{cm}, the coordinate system we use is displaced by l_{cm} from the center of mass coordinate system. Therefore, the transformation matrix between these two coordinate systems becomes (3+1)x(3+1) where the 3x3 part corresponds to the ordinary rotation whereas a row and a column are added to be able to express the displacement between the coordinate systems.

Rotation of the system about the yaw axis through an angle of α is expressed by the first rotation matrix :

$$\underline{\underline{R_1}} = \begin{bmatrix} cos(\alpha) & sin(\alpha) & 0 & 0 \\ -sin(\alpha) & cos(\alpha) & 0 & 0 \\ 0 & 0 & 1 & 0 \\ 0 & 0 & 0 & 1 \end{bmatrix} \tag{2.10}$$

Similarly, rotation of the system about the pitch axis through an angle of θ is given by the second rotation matrix :

$$\underline{\underline{R_2}} = \begin{bmatrix} cos(\theta) & 0 & -sin(\theta) & 0 \\ 0 & 1 & 0 & 0 \\ sin(\theta) & 0 & cos(\theta) & 0 \\ 0 & 0 & 0 & 1 \end{bmatrix} \tag{2.11}$$

The translation matrix shifting the pivot point to the center of mass point is written as

$$\underline{\underline{T_3}} = \begin{bmatrix} 1 & 0 & 0 & l_{cm} \\ 0 & 1 & 0 & 0 \\ 0 & 0 & 1 & 0 \\ 0 & 0 & 0 & 1 \end{bmatrix} \tag{2.12}$$

Multiplication of these three matrices gives the transformation matrix from the initial to the final coordinate system.

$$\underline{\underline{M}} = \underline{\underline{R_1}}\,\underline{\underline{R_2}}\,\underline{\underline{T_3}} \tag{2.13}$$

Carrying out the matrix multiplication, $\underline{\underline{M}}$ is computed explicitly as

$$\underline{\underline{M}} = \begin{bmatrix} cos(\alpha)\, cos(\theta) & sin(\alpha) & -cos(\alpha)\, sin(\theta) & cos(\alpha)\, cos(\theta)\, l_{cm} \\ -sin(\alpha)\, cos(\theta) & cos(\alpha) & sin(\alpha)\, sin(\theta) & -sin(\alpha)\, cos(\theta)\, l_{cm} \\ sin(\theta) & 0 & cos(\theta) & sin(\theta)\, l_{cm} \\ 0 & 0 & 0 & 1 \end{bmatrix} \tag{2.14}$$

Apart from the "1" as the last entry, the last column represents the transformed position of the center of mass after two rotations in the generalized Cartesian coordinates.

$$x_{cm} = cos(\alpha)\, cos(\theta)\, l_{cm} \tag{2.15}$$

$$y_{cm} = -sin(\alpha)\, cos(\theta)\, l_{cm} \tag{2.16}$$

$$z_{cm} = sin(\theta)\, l_{cm} \tag{2.17}$$

The components of the velocity of center of mass are found by taking the time derivative of the generalized Cartesian coordinates

$$\dot{x}_{cm} = l_{cm} \left[-\dot{\alpha}\, cos(\theta)\, sin(\alpha) - \dot{\theta} sin(\theta)\, cos(\alpha) \right] \tag{2.18}$$

$$\dot{y}_{cm} = l_{cm} \left[-\dot{\alpha}\, cos(\theta)\, cos(\alpha) + \dot{\theta} sin(\theta)\, sin(\alpha) \right] \tag{2.19}$$

$$\dot{z}_{cm} = l_{cm} \left[-\dot{\theta}\, cos(\theta) \right] \tag{2.20}$$

Substituting Equations 2.18, 2.19 and 2.20 into Equation 2.9 the translational kinetic energy is obtained to be

$$T_t = \frac{1}{2} m_{heli}\, l_{cm}^2 \left(\dot{\alpha}^2 cos^2(\theta) + \dot{\theta}^2 \right) \tag{2.21}$$

Finally, plugging Equations 2.7, 2.8 and 2.21 into Equation 2.6 gives the total kinetic energy of the helicopter system.

$$T = \frac{1}{2}\left[J_p\,\dot{\theta}^2 + J_y\,\dot{\alpha}^2 + m_{heli}\,l_{cm}^2\left(\dot{\alpha}^2 cos^2(\theta) + \dot{\theta}^2\right)\right] \tag{2.22}$$

The nonconservative forces corresponding to the generalized coordinates are torques generated by motors and friction forces. Front and tail propellers produce torques acting on both pitch and yaw axes because of the coupling effect; hence, nonconservative forces can be defined as in Equations 2.23 and 2.24.

$$Q_p = \tau_{prop\_pp} + \tau_{prop\_py} - \tau_p \tag{2.23}$$

where τ_{prop_pp} is the propulsive torque acting on pitch axis generated by front propeller, τ_{prop_py} is the propulsive torque acting on pitch axis generated by tail propeller and τ_p is the torque of the friction force on the pitch axis.

$$Q_y = \tau_{prop\_yy} + \tau_{prop\_yp} - \tau_y \tag{2.24}$$

where τ_{prop_yy} is the propulsive torque acting on yaw axis generated by tail propeller, τ_{prop_yp} is the propulsive torque acting on yaw axis generated by front propeller and τ_y is the torque of the friction force on the yaw axis. Propulsive torques are proportional to the input voltages of dc motors and can simply be defined as the product of these voltages with the corresponding torque constants [12].

$$\tau_{prop\_pp} = K_{pp}\,U_p \tag{2.25}$$

$$\tau_{prop\_py} = K_{py}\,U_y \tag{2.26}$$

$$\tau_{prop\_yy} = K_{yy}\,U_y \tag{2.27}$$

$$\tau_{prop\_yp} = K_{yp}\,U_p \tag{2.28}$$

Viscous friction constans are denoted by B_p and B_y about pitch and yaw axis respectively. Then, torque of the friction forces can be expressed as

$$\tau_p = B_p \, \dot{\theta} \tag{2.29}$$

$$\tau_y = B_y \, \dot{\alpha} \tag{2.30}$$

Using Equations 2.2, 2.3, 2.5, 2.22, 2.23, 2.25, 2.26, 2.29 and rearranging gives the following second order differential equation for the pitch axis.

$$\ddot{\theta} = \frac{K_{pp} \, U_p + K_{py} \, U_y - B_p \, \dot{\theta} - m_{heli} \, l_{cm}^2 \, \dot{\alpha}^2 \, cos(\theta) \, sin(\theta) - m_{heli} \, g \, l_{cm} \, cos(\theta)}{J_p + m_{heli} \, l_{cm}^2} \tag{2.31}$$

Similarly, substituting Equations 2.2, 2.5, 2.22, 2.24, 2.27, 2.28, 2.30 into Equation 2.4 gives the following second order differential equation for the yaw axis.

$$\ddot{\alpha} = \frac{K_{yp} \, U_p + K_{yy} \, U_y - B_y \, \dot{\alpha} + 2 \, m_{heli} \, l_{cm}^2 \, \dot{\alpha} \, \dot{\theta} \, cos(\theta) \, sin(\theta)}{J_y + m_{heli} \, l_{cm}^2 \, cos^2(\theta)} \tag{2.32}$$

Governing equations for 2-DOF-HS are coupled nonlinear differential equations and they are represented as follows

$$\begin{aligned} \frac{d}{dt} \begin{bmatrix} \theta \\ \alpha \\ \dot{\theta} \\ \dot{\alpha} \end{bmatrix} &= \begin{bmatrix} \dot{\theta} \\ \dot{\alpha} \\ \frac{-B_p \, \dot{\theta} - m_{heli} \, l_{cm}^2 \, \dot{\alpha}^2 \, cos(\theta) \, sin(\theta) - m_{heli} \, g \, l_{cm} \, cos(\theta)}{J_p + m_{heli} \, l_{cm}^2} \\ \frac{-B_y \, \dot{\alpha} + 2 \, m_{heli} \, l_{cm}^2 \, \dot{\alpha} \, \dot{\theta} \, cos(\theta) \, sin(\theta)}{J_y + m_{heli} \, l_{cm}^2 \, cos^2(\theta)} \end{bmatrix} \\ &+ \begin{bmatrix} 0 & 0 \\ 0 & 0 \\ \frac{K_{pp}}{J_p + m_{heli} \, l_{cm}^2} & \frac{K_{py}}{J_p + m_{heli} \, l_{cm}^2} \\ \frac{K_{yp}}{J_p + m_{heli} \, l_{cm}^2 \, cos^2(\theta)} & \frac{K_{yy}}{J_p + m_{heli} \, l_{cm}^2 \, cos^2(\theta)} \end{bmatrix} \begin{bmatrix} U_p \\ U_y \end{bmatrix} \end{aligned} \tag{2.33}$$

Finally, dynamics of the system is written in the compact form

$$\underline{\dot{x}} = \underline{f} \, (\underline{x}, \underline{u}) \tag{2.34}$$

where $\underline{x}^T = \begin{bmatrix} \theta & \alpha & \dot{\alpha} & \dot{\theta} \end{bmatrix}^T$ is the state vector and output variables can be chosen as

$$\underline{y} = \underline{h}(\underline{x}) = \begin{bmatrix} 1 & 0 & 0 & 0 \\ 0 & 1 & 0 & 0 \end{bmatrix} \underline{x} = \begin{bmatrix} \theta \\ \alpha \end{bmatrix} \tag{2.35}$$

2.3. Experimental Tuning of the Model Parameters

The mathematical model of the system contains various parameters that must be taken into consideration. They can be calculated theoretically or determined experimentally. Most of the parameters are taken from the user's manual of 2-DOF Helicopter System [1]. However, some of the parameters are found to be wrong or untrustworthy. Hence, they were calibrated in order to be able to control the system properly.

3. THEORETICAL BACKGROUND

3.1. Full State Feedback Control via LQR

FSFC is a fundamental approach to control a linear-time-varying or linear-time independent system. The idea behind this method is to multiply all state variables by an appropriate vector or matrix and apply the result to the system as a control input. This multiplying vector or matrix can be found using LQR algorithm. Consider an LTI system in state-space form

$$\dot{\underline{x}} = \underline{\underline{A}}\,\underline{x} + \underline{\underline{B}}\,\underline{u} \tag{3.1}$$

$$\underline{y} = \underline{\underline{C}}\,\underline{x} + \underline{\underline{D}}\,\underline{u} \tag{3.2}$$

where $\underline{\underline{A}} \in \Re^{nxn}$ is the system matrix, $\underline{\underline{B}} \in \Re^{nxm}$ is the input matrix, $\underline{\underline{C}} \in \Re^{rxn}$ is the output matrix, $\underline{\underline{D}} \in \Re^{rxm}$ is the feedthrough matrix, $\underline{x} \in \Re^{n}$ is the state vector , $\underline{y} \in \Re^{r}$ is the output vector and $\underline{u} \in \Re^{m}$ is the input vector. It is assumed that all the state variables are available for the feedback. The control law for the regulation problem where there is no reference input is $\underline{u} = -\underline{\underline{K}}\,\underline{x}$. If there is a reference trajectory $\underline{x}_d \in \Re^{m}$ to track, integrators can be used to obtain zero steady-state error. Hence, state-space equations are augmented by two integrators [13].

$$\dot{\hat{\underline{x}}} = \underline{\underline{\hat{A}}}\,\hat{\underline{x}} + \underline{\underline{\hat{B}}}\,\underline{u} - \underline{\underline{W}}\,\underline{x}_d \tag{3.3}$$

$$\underline{y} = \underline{\underline{\hat{C}}}\,\hat{\underline{x}} + \underline{\underline{D}}\,\underline{u} \tag{3.4}$$

where,

$$\underline{\underline{\hat{A}}} = \begin{bmatrix} \underline{\underline{A}} & \underline{\underline{0}} \\ \underline{\underline{C}} & \underline{\underline{0}} \end{bmatrix} \tag{3.5}$$

$$\underline{\underline{\hat{B}}} = \begin{bmatrix} \underline{\underline{B}} \\ \underline{\underline{0}} \end{bmatrix} \tag{3.6}$$

$$\underline{\underline{W}} = \begin{bmatrix} \underline{\underline{0}} \\ \underline{\underline{I}} \end{bmatrix} \tag{3.7}$$

$$\underline{\hat{x}} = \begin{bmatrix} \underline{x} \\ \underline{x}_I \end{bmatrix} \tag{3.8}$$

In Equation 3.8, $\underline{x}_I$ is defined as follows:

$$\underline{x}_I = \begin{bmatrix} \int_0^t (x_1 - x_{1d})\, dt \\ \int_0^t (x_2 - x_{2d})\, dt \end{bmatrix} \tag{3.9}$$

The new control law can be defined as follows:

$$\underline{u} = -\underline{\underline{\hat{K}}}\, \underline{\tilde{x}} \tag{3.10}$$

where $\underline{\tilde{x}} = \underline{x} - \underline{x}_d$ and $\underline{\underline{\hat{K}}}$ is the new gain matrix.

If the augmented system is completely state controllable, the gain matrix $\underline{\underline{\hat{K}}}$ is always determined in such a way that all the eigenvalues of $\underline{\underline{\hat{A}}} - \underline{\underline{\hat{B}}}\,\underline{\underline{\hat{K}}}$ are negative [14]. This gain matrix can be designed with either pole-placement method or LQR algorithm. In this thesis, LQR algorithm is used in order to find the gain matrix with the following performance index [15]

$$J = \int_0^{\infty} (\underline{\tilde{x}}^T \underline{\underline{Q}}\, \underline{\tilde{x}} + \underline{u}^T \underline{\underline{R}}\, \underline{u})\, dt \tag{3.11}$$

where $\underline{\underline{Q}} \in \Re^{nxn}$ and $\underline{\underline{R}} \in \Re^{mxm}$ are both positive-definite symmetric matrices and $\underline{u}$ is unconstrained. Although there is not any systematic way to choose the values for the entries of $\underline{\underline{Q}}$ and $\underline{\underline{R}}$, these values can be selected after a number of trials. Minimum of the performance index is obtained when [15]

$$\underline{\underline{\hat{K}}} = \underline{\underline{R}}^{-1}\underline{\underline{\hat{B}}}^T\underline{\underline{P}} \tag{3.12}$$

where $\underline{\underline{P}}$ is found from the solution of the so called Riccati Equation [15].

$$\underline{\underline{\hat{A}}}^T\underline{\underline{P}} + \underline{\underline{P}}\,\underline{\underline{\hat{A}}} - \underline{\underline{P}}\,\underline{\underline{\hat{B}}}\,\underline{\underline{R}}^{-1}\underline{\underline{\hat{B}}}^T\underline{\underline{P}} + \underline{\underline{Q}} = 0 \tag{3.13}$$

3.2. Feedback Linearization

Feedback Linearization uses algebraic methods to linearize a set of nonlinear equations of a system in order to apply linear control techniques. Consider a square system which has the same number of input and output entries with the following representation [2]

$$\dot{\underline{x}} = \underline{f}(\underline{x}) + \underline{\underline{G}}(\underline{x})\,\underline{u} \tag{3.14}$$

$$\underline{y} = \underline{h}(\underline{x}) \tag{3.15}$$

where $\underline{x} \in \Re^n$ is the state vector, $\underline{u} \in \Re^m$ is the control input vector, $\underline{y} \in \Re^m$ the output vector, $\underline{f}$ and $\underline{g}$ are smooth vector fields and $\underline{\underline{G}} \in \Re^{nxm}$ is a matrix whose columns are smooth vector fields g_i. In order to apply input-output linearization to a MIMO system, time derivatives of the entries of the output vector are taken until the inputs appear. This operation can be represented in the Lie algebra as [2]

$$y_i^{(r_i)} = L_{\underline{f}}^{r_i}\, h_i + \sum_{j=1}^{m} L_{\underline{g}_j}\, L_{\underline{f}}^{r_i - 1}\, h_i\, u_j \tag{3.16}$$

where L denotes the Lie derivative operator. If r_j is the minimum integer which causes at least one of the inputs takes part in $y_i^{(r_i)}$, then the following equation holds for at least one j [2]

$$L_{\underline{g}_j} L_{\underline{f}}^{r_i-1} h_i(\underline{x}) \neq 0 \tag{3.17}$$

Time derivatives of the outputs can be expressed as [2]

$$\begin{bmatrix} y_i^{(r_1)} \\ \cdots \\ \cdots \\ y_m^{(r_m)} \end{bmatrix} = \begin{bmatrix} L_{\underline{f}}^{r_1} h_1(\underline{x}) \\ \cdots \\ \cdots \\ L_{\underline{f}}^{r_m} h_m(\underline{x}) \end{bmatrix} + \underline{\underline{E}}(\underline{x})(\underline{u}) \tag{3.18}$$

where $\underline{\underline{E}}(\underline{x}) \in \Re^{mxm}$. If $\underline{\underline{E}}(\underline{x})$ is invertable, then $\underline{u}$ can be defined as follows [2]

$$\underline{u} = \underline{\underline{E}}^{-1} \begin{bmatrix} v_1 - L_{\underline{f}}^{r_1} h_1 \\ \cdots \\ \cdots \\ v_m - L_{\underline{f}}^{r_m} h_m \end{bmatrix} \tag{3.19}$$

Substituting Equation 3.19 into Equation 3.18 yields m number of simple equations [2]

$$y_i^{r_i} = v_i \qquad i = 1, 2, \ldots, m \tag{3.20}$$

Now, one of the linear control approaches can be applied.

3.3. Sliding Mode Control

Sliding Mode Control is a kind of robust control which deals with uncertain systems. This methodology defines 1st order systems and solves them regardless of the degree of the original system. Consider a MIMO system with a set of nonlinear equations [2]

$$x_i^{(n_i)} = f_i(\underline{x}) + \sum_{j=1}^{m} b_{ij}\, u_j \qquad i = 1, \ldots, m \qquad j = 1, \ldots, m \tag{3.21}$$

where input vector $\underline{x}$ consists of x_i's and their first $n_i - 1$ derivatives and

$$\underline{u}^T = [u_1, \ldots, u_m]^T \tag{3.22}$$

$$\underline{f}(\underline{x})^T = [f_1(\underline{x}), \ldots, f_m(\underline{x})]^T \tag{3.23}$$

$$\underline{\underline{B}}(\underline{x}) = \begin{bmatrix} b_{11}(\underline{x}) & \cdots & b_{1m}(\underline{x}) \\ \vdots & \ddots & \vdots \\ b_{m1}(\underline{x}) & \cdots & b_{mm}(\underline{x}) \end{bmatrix} \tag{3.24}$$

The aim of the methodology is to track a desired trajectory $\underline{x}_d$ while $\underline{f}(\underline{x})$ and $\underline{\underline{B}}(\underline{x})$ have uncertainty. The uncertainty on $\underline{f}(\underline{x})$ is bounded as follows [2]

$$\left| f_i - \hat{f}_i \right| \leq F_i \qquad i = 1, \ldots, m \tag{3.25}$$

where $\hat{f}_i$ which is the estimated value of f_i can be defined simply as

$$\hat{f}_i = \frac{\max\{f_i\} + \min\{f_i\}}{2} \tag{3.26}$$

F_i takes its maximum value when

$$F_i = \left| \hat{f}_i - \min\{f_i\} \right| \tag{3.27}$$

The entries of $\underline{\underline{B}}$ are bounded as

$$\min\{b_{ij}\} \leq b_{ij} \leq \max\{b_{ij}\} \qquad i = 1, \ldots, m \qquad j = 1, \ldots, m \tag{3.28}$$

and the relation between the nominal and the estimated input matrix is [2]

$$\underline{\underline{B}} = (\underline{\underline{I}} + \underline{\underline{\Delta}})\underline{\underline{\hat{B}}} \tag{3.29}$$

where $\underline{\underline{\hat{B}}}$ is the estimated input matrix, $\underline{\underline{\Delta}}$ is the uncertainty matrix and $\underline{\underline{I}} \in \Re^{nxn}$ is the identity matrix. The entries of the uncertainty matrix are bounded from above and below as follows [2]

$$|\Delta_{ij}| \leq D_{ij} \tag{3.30}$$

On the other hand, the estimated input matrix is obtained by the following steps. Consider the special case in which the entries of the input matrix are independent of each other. Then, $\forall i, j \;\; i \neq j \;\; \Delta_{ij} = 0$ and Equation 3.29 becomes

$$b_{ij} = (1 + \Delta_{ii})\,\hat{b}_{ij} \tag{3.31}$$

The values of the entries of $\underline{\underline{\hat{B}}}$ can be defined as the geometric mean of the maximum and the minimum values of b_{ij}

$$\hat{b}_{ij} = \sqrt{\max\{b_{ij}\}\,\min\{b_{ij}\}} \tag{3.32}$$

Using Equations 3.28, 3.31, 3.32 and rearranging leads to

$$\beta_{ij}^{-1} \leqslant (1 + \Delta_{ii}) \leq \beta_{ij} \tag{3.33}$$

where,

$$\beta_{ij} = \sqrt{\frac{\max\{b_{ij}\}}{\min\{b_{ij}\}}} \tag{3.34}$$

and Δ_{ii}'s are bounded as follows

$$\max\{\Delta_{ii}\} = |\max\{\beta_{ij} - 1\}| \tag{3.35}$$

Although there are various ways of designing sliding surfaces s_i, the following definition is chosen [2]

$$s_i = (\frac{d}{dt} + \lambda_i)^{n_i - 1}\,\tilde{x}_i \tag{3.36}$$

$$\tilde{x}_i = x_{di} - x_i \tag{3.37}$$

where $\tilde{x}$ is the tracking error and λ_i are strictly positive numbers. Integral control can be used by adding 1 to n_i [2]. In order to simplify the calculations, a new vector x_r is defined as [2]

$$\underline{x}_r = \begin{bmatrix} x_{r1} \\ \vdots \\ x_{rn} \end{bmatrix} \tag{3.38}$$

$$x_{ri}^{(n_i-1)} = x_i^{(n_i-1)} - s_i \qquad i = 1, \ldots, n \tag{3.39}$$

Assume $\underline{\underline{\hat{B}}}$ is invertible, then the control law can be designed as

$$\underline{u} = \underline{\underline{\hat{B}}}^{-1}\left[\underline{x}_r^{(n)} - \underline{\hat{f}}(\underline{x}) - \underline{z}(\underline{s})\right] \tag{3.40}$$

with,

$$\underline{z}(\underline{s})^T = [k_1 sgn(s_1), \ldots, k_n sgn(s_n)]^T$$

where $sgn(.)$ is the signum function. k_i's are selected in order to make the sliding surface an invariant set,

$$k_i = \frac{F_i + D_{ii} \max\left\{x_{ri}^{(n)} - \hat{f}_i\right\} + \eta_i}{1 - D_{ii}} \tag{3.41}$$

where η_i are strictly positive constants and they decide how fast the system trajectories move toward the sliding surface. Choosing the k_i's as in the equation above, the squared distances between the system trajectory and the sliding surfaces decreases as time flows which can be expressed by the following equation [2].

$$\frac{1}{2}\frac{d}{dt}s_i \leq -\eta_i \left|s_i\right| \qquad \eta_i > 0 \tag{3.42}$$

Although the control law given in Equation 3.40 provides zero steady-state error, it causes chattering because it is discontinous across the surface. One method to reduce chattering is smoothing out the control discontinuity in a boundary layer [2]. Hence, $\underline{z}(\underline{s})^T$ in the control law is modified as follows

$$\underline{z}(\underline{s})^T = [k_1 sat(s_1/\phi_1), \ldots, k_n sat(s_n/\phi_n)]^T \qquad \forall i \qquad \phi_i > 0$$

where ϕ is the boundary layer thickness and sat is the saturation function:

$$sat(f) = f \qquad\qquad if\,|f| \leq 1 \tag{3.43}$$

$$sat(f) = sgn(f) \qquad\qquad otherwise \tag{3.44}$$

Even though there is not any systematic way to determine the boundary layer thickness, it must be chosen as small as possible because it increases the steady-state error.

4. DESIGN AND IMPLEMENTATION OF THE CONTROL METHODOLOGIES

In this thesis, the main approach to control Q-2-DOF-HS is SMC. This methodology is suitable for this system because it deals with modeling inaccuracies, external disturbances and uncertainties. FSFC is a basic and widespread approach and it is applied to the system. This methodology is also given in the manual of the experimental setup [16]. Moreover, a common nonlinear control approach, FL, is used to control the helicopter system for comparison. For implementation of these methodologies to the helicopter system there are some limitations have to be taken into account. Pitch angle of the helicopter is mechanically constrained between ± 40 degrees. Input voltages, which are applied to the main and tail motors, are limited between ± 24 and ± 15 using saturation blocks in the controllers [1]. In addition, all the state variables of the system need to be measured. Although the helicopter system does not have tachometers to measure angular velocities, these variables can be obtained by differentiating the pitch and yaw angles with in the computer environment. Differentiation process is handled by the second order low pass filter given by the manufacturer. SMC and FL controllers use the time derivative of the reference trajectory and this value becomes too large for a step or square-wave inputs. Therefore, a continous nonlinear filter is implemented for smoothing the input commands [17]. This filter is designed using SMC and it has three parameters to be chosen which are the first and second derivative bounds of the input and the boundary layer constant. The boundary layer constant of the filter is set to 2 experimentally and the bounds of the inputs are determined in Chapter 4.3.

4.1. Full-State Feedback Control via LQR

Nonlinear differential equations of the system have to be linearized in order to apply FSFC. Local linearization is a basic method for linearizing the equations. This operation can be utilized by Taylor expansion around the origin of the system. All the state variables of the system are available for the feedback. The equations of the system is written in the following form

$$\underline{\dot{x}} = \underline{f}(\underline{x}) + \underline{g}(\underline{x})\,\underline{u} \tag{4.1}$$

where $\underline{x}^T$ is the state vector, $\underline{u}^T$ is the input vector, $\underline{f}(\underline{x})$ and $\underline{g}(\underline{x})$ is defined as follows

$$\underline{f}(\underline{x}) = \begin{bmatrix} \dot{\theta} \\ \dot{\alpha} \\ \frac{-B_p\,\dot{\theta} - m_{heli}\,l_{cm}^2\,\dot{\alpha}^2\,cos(\theta)\,sin(\theta) - m_{heli}\,g\,l_{cm}\,cos(\theta)}{J_p + m_{heli}\,l_{cm}^2} \\ \frac{-B_y\,\dot{\alpha} + 2\,m_{heli}\,l_{cm}^2\,\dot{\alpha}\,\dot{\theta}\,cos(\theta)\,sin(\theta)}{J_y + m_{heli}\,l_{cm}^2\,cos^2(\theta)} \end{bmatrix} \tag{4.2}$$

$$\underline{g}(\underline{x}) = \begin{bmatrix} 0 & 0 \\ 0 & 0 \\ \frac{K_{pp}}{J_p + m_{heli}\,l_{cm}^2} & \frac{K_{yp}}{J_p + m_{heli}\,l_{cm}^2} \\ \frac{K_{py}}{J_y + m_{heli}\,l_{cm}^2\,cos^2(\theta)} & \frac{K_{yy}}{J_y + m_{heli}\,l_{cm}^2\,cos^2(\theta)} \end{bmatrix} \tag{4.3}$$

Equation 4.1 is expanded in Taylor series

$$\underline{\dot{x}}(\underline{x}, \underline{u}) = \underline{f}(\underline{x}_{eq}, \underline{u}_{eq}) + \underline{f}_{\underline{x}}(\underline{x}_{eq}, \underline{u}_{eq})(\underline{x} - \underline{x}_{eq}) + \underline{g}_{\underline{u}}(\underline{x}_{eq}, \underline{u}_{eq})\,(\underline{u} - \underline{u}_{eq}) + H.O.T. \tag{4.4}$$

where the equilibrium point of the system is $\underline{x}_{eq} = \underline{0}$ when $\underline{u}_{eq}^T = [U_{eq\text{-}p}\,U_{eq\text{-}y}]$. Hence, $\underline{x}$ and $\underline{u}$ are replaced by $\underline{x}_{eq}$ and $\underline{u}_{eq}$ respectively in Equation 4.1 to find the equilibrium control inputs.

$$\underline{\dot{x}}(\underline{x}_{eq}, \underline{u}_{eq}) = \begin{bmatrix} 0 \\ 0 \\ -\frac{m_{heli}\,g\,l_{cm}}{J_p + m_{heli}\,l_{cm}^2} \\ 0 \end{bmatrix} + \begin{bmatrix} 0 & 0 \\ 0 & 0 \\ \frac{K_{pp}}{J_p + m_{heli}\,l_{cm}^2} & \frac{K_{py}}{J_p + m_{heli}\,l_{cm}^2} \\ \frac{K_{yp}}{J_y + m_{heli}\,l_{cm}^2} & \frac{K_{yy}}{J_y + m_{heli}\,l_{cm}^2} \end{bmatrix} \begin{bmatrix} U_{eq\text{-}p} \\ U_{eq\text{-}y} \end{bmatrix} = 0 \tag{4.5}$$

Solving the equation above, $U_{eq\text{-}p}$ and $U_{eq\text{-}y}$ are obtained as follows

$$U_{eq\text{-}p} = \frac{K_{yy}}{K_{pp}\,K_{yy} - K_{py}\,K_{yp}}\,m_{heli}\,g\,l_{cm} \tag{4.6}$$

$$U_{eq\text{-}y} = -\frac{K_{yp}}{K_{pp}\,K_{yy} - K_{py}\,K_{yp}}\,m_{heli}\,g\,l_{cm} \tag{4.7}$$

Jacobians of $\underline{f}(\underline{x})$ and $\underline{g}(\underline{x})$ at $\underline{x}_{eq} = \underline{0}$ and $\underline{u}_{eq}^T = [U_{eq\text{-}p}\,U_{eq\text{-}y}]^T$ give the linearized equations of motions of the helicopter system.

$$\begin{aligned}\dot{\underline{x}} &= \begin{bmatrix} 0 & 0 & 1 & 0 \\ 0 & 0 & 0 & 1 \\ 0 & 0 & -\frac{B_p}{J_p + m_{heli}\,l_{cm}^2} & 0 \\ 0 & 0 & 0 & -\frac{B_y}{J_y + m_{heli}\,l_{cm}^2} \end{bmatrix} \underline{x} \\ &+ \begin{bmatrix} 0 & 0 \\ 0 & 0 \\ \frac{K_{pp}}{J_p + m_{heli}\,l_{cm}^2} & \frac{K_{py}}{J_p + m_{heli}\,l_{cm}^2} \\ \frac{K_{yp}}{J_y + m_{heli}\,l_{cm}^2} & \frac{K_{yy}}{J_y + m_{heli}\,l_{cm}^2} \end{bmatrix} \underline{u} + \begin{bmatrix} 0 \\ 0 \\ \frac{K_{yy}}{K_{pp}\,K_{yy} - K_{py}\,K_{yp}}\,m_{heli}\,g\,l_{cm} \\ -\frac{K_{yp}}{K_{pp}\,K_{yy} - K_{py}\,K_{yp}}\,m_{heli}\,g\,l_{cm} \end{bmatrix}\end{aligned} \tag{4.8}$$

The system matrix $\underline{\underline{A}}$ and the input matrix $\underline{\underline{B}}$ for the helicopter system is

$$\underline{\underline{A}} = \begin{bmatrix} 0 & 0 & 1 & 0 \\ 0 & 0 & 0 & 1 \\ 0 & 0 & -\frac{B_p}{J_p + m_{heli}\,l_{cm}^2} & 0 \\ 0 & 0 & 0 & -\frac{B_y}{J_y + m_{heli}\,l_{cm}^2} \end{bmatrix} \tag{4.9}$$

$$\underline{\underline{B}} = \begin{bmatrix} 0 & 0 \\ 0 & 0 \\ \frac{K_{pp}}{J_p + m_{heli}\,l_{cm}^2} & \frac{K_{yp}}{J_p + m_{heli}\,l_{cm}^2} \\ \frac{K_{py}}{J_y + m_{heli}\,l_{cm}^2} & \frac{K_{yy}}{J_y + m_{heli}\,l_{cm}^2} \end{bmatrix} \tag{4.10}$$

Pitch and yaw angles are chosen as output variables. Hence, $\underline{\underline{C}}$ and $\underline{\underline{D}}$ matrices are

$$\underline{\underline{C}} = \begin{bmatrix} 1 & 0 & 0 & 0 \\ 0 & 1 & 0 & 0 \end{bmatrix} \qquad \underline{\underline{D}} = \underline{\underline{0}} \tag{4.11}$$

Using Equations 3.5, 3.6 and 3.7 $\underline{\underline{\hat{A}}}$, $\underline{\underline{\hat{B}}}$ and $\underline{\underline{W}}$ are obtained as follows:

$$\underline{\underline{\hat{A}}} = \begin{bmatrix} 0 & 0 & 1 & 0 & 0 & 0 \\ 0 & 0 & 0 & 1 & 0 & 0 \\ 0 & 0 & -\frac{B_p}{J_p+m_{heli}\,l_{cm}^2} & 0 & 0 & 0 \\ 0 & 0 & 0 & -\frac{B_y}{J_y+m_{heli}\,l_{cm}^2} & 0 & 0 \\ 1 & 0 & 0 & 0 & 0 & 0 \\ 0 & 1 & 0 & 0 & 0 & 0 \end{bmatrix} \tag{4.12}$$

$$\underline{\underline{\hat{B}}} = \begin{bmatrix} 0 & 0 \\ 0 & 0 \\ \frac{K_{pp}}{J_p+m_{heli}\,l_{cm}^2} & \frac{K_{yp}}{J_p+m_{heli}\,l_{cm}^2} \\ \frac{K_{py}}{J_y+m_{heli}\,l_{cm}^2} & \frac{K_{yy}}{J_y+m_{heli}\,l_{cm}^2} \\ 0 & 0 \\ 0 & 0 \end{bmatrix} \tag{4.13}$$

$$\underline{\underline{W}} = \begin{bmatrix} 0 & 0 \\ 0 & 0 \\ 0 & 0 \\ 0 & 0 \\ 1 & 0 \\ 0 & 1 \end{bmatrix} \tag{4.14}$$

Controllability of the system is specified by the rank of the controllability matrix. This matrix is obtained by using the O=ctrb(A,B) command of the MATLAB. In this command, A denotes $\underline{\underline{\hat{A}}}$ and B denotes $\underline{\underline{\hat{B}}}$

$$\underline{\underline{Q}} = c* \begin{bmatrix} 0 & 0 & 0 & 0 & 0 & 0 & 0 & 0 & 0 & 0 & 0 & 0 \\ 0 & 0 & 0 & 0 & -0.1 & -0.2 & 1.1 & 2.1 & -13 & -25 & 15 & 29 \\ 0 & 0 & 0 & 0 & 0 & 0 & 0 & 0 & 0 & 0 & 0 & 0 \\ 0 & 0 & -0.1 & -0.2 & 1.1 & 2.1 & -13 & -25 & 150 & 294 & -1770 & -3450 \\ 0 & 0 & 0 & 0 & 0 & 0 & 0 & 0 & 0 & 0 & 0 & 0 \\ 0 & 0 & 0 & 0 & 0 & 0 & -0.1 & -0.2 & 1.1 & 2.1 & -13 & -25 \end{bmatrix}$$

where $c = 10^2$. Since the above matrix is full rank, the system is controllable implying that we can find an appropriate gain matrix $\underline{\underline{\hat{K}}}$ to make the system stable. $\underline{\underline{R}}$ and $\underline{\underline{Q}}$ matrices are constructed to find optimal gain matrix. $\underline{\underline{R}}$ is set to be identity matrix and $\underline{\underline{Q}}$ is designed by trial and error such that control input does not exceed the maximum voltage limits [1].

$$\underline{\underline{R}} = \begin{bmatrix} 1 & 0 \\ 0 & 1 \end{bmatrix} \tag{4.15}$$

$$\underline{\underline{Q}} = \begin{bmatrix} 40 & 0 & 0 & 0 & 0 & 0 \\ 0 & 60 & 0 & 0 & 0 & 0 \\ 0 & 0 & 30 & 0 & 0 & 0 \\ 0 & 0 & 0 & 30 & 0 & 0 \\ 0 & 0 & 0 & 0 & 10 & 0 \\ 0 & 0 & 0 & 0 & 0 & 32 \end{bmatrix} \tag{4.16}$$

Since $\underline{\underline{\hat{A}}}$, $\underline{\underline{\hat{B}}}$, $\underline{\underline{Q}}$ and $\underline{\underline{R}}$ matrices are obtained, gain matrix $\underline{\underline{\hat{K}}}$, which is the solution of Equation 3.13 is computed by lqr command of MATLAB software.

$$[K,\, P,\, E] = lqr(A,\, B,\, Q,\, R) \tag{4.17}$$

4.2. Feedback Linearization

The dynamics of the helicopter is represented by Equations 3.14 and 3.15.

$$\underline{\dot{x}} = \underbrace{\begin{bmatrix} \dot{\theta} \\ \dot{\alpha} \\ \frac{-B_p\,\dot{\theta} - m_{heli}\,l_{cm}^2\,\dot{\alpha}^2\,cos(\theta)\,sin(\theta) - m_{heli}\,g\,l_{cm}\,cos(\theta)}{J_p + m_{heli}\,l_{cm}^2} \\ \frac{-B_y\,\dot{\alpha} + 2\,m_{heli}\,l_{cm}^2\,\dot{\alpha}\,\dot{\theta}\,cos(\theta)\,sin(\theta)}{J_y + m_{heli}\,l_{cm}^2\,cos^2(\theta)} \end{bmatrix}}_{\underline{f}(\underline{x})}$$

$$+ \underbrace{\begin{bmatrix} 0 & 0 \\ 0 & 0 \\ \frac{K_{pp}}{J_p + m_{heli}\,l_{cm}^2} & \frac{K_{py}}{J_p + m_{heli}\,l_{cm}^2} \\ \frac{K_{yp}}{J_p + m_{heli}\,l_{cm}^2\,cos^2(\theta)} & \frac{K_{yy}}{J_p + m_{heli}\,l_{cm}^2\,cos^2(\theta)} \end{bmatrix}}_{\underline{\underline{G}}(\underline{x})} \underline{u} \tag{4.18}$$

$$\underline{y} = \underline{h}(\underline{x}) = \begin{bmatrix} h_1(\underline{x}) \\ h_2(\underline{x}) \end{bmatrix} = \begin{bmatrix} \theta \\ \alpha \end{bmatrix} \tag{4.19}$$

The Lie derivatives of the outputs with respect to $\underline{f}(\underline{x})$ and $\underline{g}(\underline{x})$ are

$$L_{\underline{f}}\,\underline{h}(\underline{x}) = \begin{bmatrix} \dot{\theta} \\ \dot{\alpha} \end{bmatrix} \tag{4.20}$$

$$L_{\underline{g}}\,\underline{h}(\underline{x}) = \underline{0} \tag{4.21}$$

Since $L_{\underline{g}}\,\underline{h}(\underline{x})$ does not include any input, the outputs are differentiated again.

$$L_{\underline{f}}^2\,\underline{h}(\underline{x}) = \begin{bmatrix} \frac{-B_p\,\dot{\theta} - m_{heli}\,l_{cm}^2\,\dot{\alpha}^2\,cos(\theta)\,sin(\theta) - m_{heli}\,g\,l_{cm}\,cos(\theta)}{J_p + m_{heli}\,l_{cm}^2} \\ \frac{-B_y\,\dot{\alpha} + 2\,m_{heli}\,l_{cm}^2\,\dot{\alpha}\,\dot{\theta}\,cos(\theta)\,sin(\theta)}{J_y + m_{heli}\,l_{cm}^2\,cos^2(\theta)} \end{bmatrix} \tag{4.22}$$

$$L_{\underline{g}}\,L_{\underline{f}}\,\underline{h}(\underline{x}) = \begin{bmatrix} \frac{K_{pp}}{J_p + m_{heli}\,l_{cm}^2} & \frac{K_{py}}{J_p + m_{heli}\,l_{cm}^2} \\ \frac{K_{yp}}{J_y + m_{heli}\,l_{cm}^2\,cos^2(\theta)} & \frac{K_{yy}}{J_y + m_{heli}\,l_{cm}^2\,cos^2(\theta)} \end{bmatrix} \tag{4.23}$$

The second derivatives of the outputs can be expressed as

$$\ddot{y} = \begin{bmatrix} \ddot{\theta} \\ \ddot{\alpha} \end{bmatrix} = \begin{bmatrix} L_{\underline{f}}^2 h_1(\underline{x}) \\ L_{\underline{f}}^2 h_2(\underline{x}) \end{bmatrix} + \underline{\underline{E}}(\underline{x})\, \underline{u} \tag{4.24}$$

where $\underline{\underline{E}}(\underline{x}) = L_{\underline{g}} L_{\underline{f}} \underline{h}(\underline{x})$. All the inputs appear in the second derivatives of the outputs; hence, there is no need to take any more derivatives and the input vector finally becomes

$$\underline{u} = \begin{bmatrix} U_p \\ U_y \end{bmatrix} = \underline{\underline{E}}^{-1} \begin{bmatrix} v_1 - L_{\underline{f}}^2 h_1 \\ v_2 - L_{\underline{f}}^2 h_2 \end{bmatrix} \tag{4.25}$$

Taking the inverse of $\underline{\underline{E}}(\underline{x})$ and using it in Equation 4.25 yields

$$\underline{u} = \begin{bmatrix} \frac{K_{yy}\,(J_p + m_{heli}\, l_{cm}^2)}{K_{pp}\,K_{yy} - K_{py}\,K_{yp}} \left[v_1 - L_{\underline{f}}^2\, \underline{h}_1\right] - \frac{K_{yy}\,(J_y + m_{heli}\, l_{cm}^2\, cos^2(\theta))}{K_{pp}\,K_{yy} - K_{py}\,K_{yp}} \left[v_2 - L_{\underline{f}}^2\, \underline{h}_2\right] \\ \frac{K_{yp}\,(J_p + m_{heli}\, l_{cm}^2)}{K_{pp}\,K_{yy} - K_{py}\,K_{yp}} \left[v_1 - L_{\underline{f}}^2\, \underline{h}_1\right] - \frac{K_{pp}\,(J_y + m_{heli}\, l_{cm}^2\, cos^2(\theta))}{K_{pp}\,K_{yy} - K_{py}\,K_{yp}} \left[v_2 - L_{\underline{f}}^2\, \underline{h}_2\right] \end{bmatrix} \tag{4.26}$$

Finally, substituting Equation 4.26 into Equation 4.24 yields

$$\underline{\ddot{y}} = \begin{bmatrix} \ddot{\theta} \\ \ddot{\alpha} \end{bmatrix} = \begin{bmatrix} v_1 \\ v_2 \end{bmatrix} \tag{4.27}$$

Since sum of the partial relative degrees is equal to the number of state variables, there is no internal dynamics [2].

$$r_t = r_1 + r_2 = 2 + 2 = 4 = n \tag{4.28}$$

Now, pole placement can be used to control the system. Thus, v_1 and v_2 are chosen so as to make the system asymptotically stable.

$$v_1 = \ddot{\theta}_d - k_{p1}(\dot{\theta} - \dot{\theta}_d) - k_{p2}(\theta - \theta_d) - k_{p3} \int_0^t (\theta - \theta_d)\, dt \tag{4.29}$$

$$v_2 = \ddot{\alpha}_d - k_{y1}(\dot{\alpha} - \dot{\alpha}_d) - k_{y2}(\alpha - \alpha_d) - k_{y3} \int_0^t (\alpha - \alpha_d)\, dt \tag{4.30}$$

Substituting Equations 4.29, 4.30 into Equation 4.27 and choosing positive values for k_{p1}, k_{p2}, k_{p3}, k_{y1}, k_{y2} and k_{y3} ensures the stability of the system. Poles are placed to damp the errors as fast as possible with trial and error while the maximum voltage limits are taken into consideration and are not exceeded [1].

Table 4.1. Values of the pole placement constants.

k_{p1}	16
k_{p2}	10
k_{p3}	7
k_{y1}	16
k_{y2}	10
k_{y3}	3

4.3. Sliding Mode Control

The helicopter system is represented by Equation 3.21. Thus, $\underline{x}$, $\underline{f}(\underline{x})$, $\underline{\underline{B}}(\underline{x})$ are expressed as follows

$$\underline{x}^T = \begin{bmatrix}\theta\,\alpha\,\dot{\theta}\,\dot{\alpha}\end{bmatrix}^T \tag{4.31}$$

$$\underline{f}(\underline{x}) = \begin{bmatrix} \frac{-B_p\,\dot{\theta} - m_{heli}\,l_{cm}^2\,\dot{\alpha}^2\,cos(\theta)\,sin(\theta) - m_{heli}\,g\,l_{cm}\,cos(\theta)}{J_p + m_{heli}\,l_{cm}^2} \\ \frac{-B_y\,\dot{\alpha} + 2\,m_{heli}\,l_{cm}^2\,\dot{\alpha}\,\dot{\theta}\,cos(\theta)\,sin(\theta)}{J_y + m_{heli}\,l_{cm}^2\,cos^2(\theta)} \end{bmatrix} \tag{4.32}$$

$$\underline{\underline{B}}(\underline{x}) = \begin{bmatrix} b_{11} & b_{12} \\ b_{21} & b_{22} \end{bmatrix} = \begin{bmatrix} \frac{K_{pp}}{J_p + m_{heli}\,l_{cm}^2} & \frac{K_{yp}}{J_p + m_{heli}\,l_{cm}^2} \\ \frac{K_{py}}{J_y + m_{heli}\,l_{cm}^2\,cos^2(\theta)} & \frac{K_{yy}}{J_y + m_{heli}\,l_{cm}^2\,cos^2(\theta)} \end{bmatrix} \tag{4.33}$$

The maximum and the minimum values of the mass of the helicopter and the location of the center of mass are taken into consideration in order to find $\hat{f}_1$ and $\hat{f}_2$.

$$m_{heli\_min} = m_{heli} \tag{4.34}$$

$$m_{heli\_max} = m_{heli} + m_{load\_max} \tag{4.35}$$

where $m_{load\_max} = 0.1$ kg is the maximum mass for the experiment. When the additional load is added to the opposite side of the center of mass, l_{cm} takes its minimum value and when there is no load, it takes its maximum value.

$$l_{cm\_max} = l_{cm} \tag{4.36}$$

$$l_{cm\_min} = \frac{l_{cm}\, m_{heli} - l_{load}\, m_{load\_max}}{m_{heli} + m_{load\_max}} \tag{4.37}$$

where $l_{load} = 0.13$m is the distance between the pivot and the location of the load. The maximum value of f_1 corresponds to the minimum values of m_{heli} and l_{cm}

$$\max\{f_1\} = \frac{-B_p\,\dot{\theta} - m_{heli\_min}\, l_{cm\_min}^2\, \dot{\alpha}^2\, cos(\theta)\, sin(\theta) - m_{heli\_min}\, g\, l_{cm\_min}\, cos(\theta)}{J_p + m_{heli\_min}\, l_{cm\_min}^2} \tag{4.38}$$

and the minimum value of f_1 corresponds to the maximum values of m_{heli} and l_{cm}

$$\min\{f_1\} = \frac{-B_p\,\dot{\theta} - m_{heli\_max}\, l_{cm\_max}^2\, \dot{\alpha}^2\, cos(\theta)\, sin(\theta) - m_{heli\_max}\, g\, l_{cm\_max}\, cos(\theta)}{J_p + m_{heli\_max}\, l_{cm\_max}^2} \tag{4.39}$$

Then, $\hat{f}_1$ is obtained using Equation 3.26 and using the constans given in Appendix B.

$$\hat{f}_1 = -0.9647\,\dot{\theta} - 0.0749\,\dot{\alpha}^2\, cos(\theta)\, sin(\theta) - 15.6651\, cos(\theta) \tag{4.40}$$

Using Equation 3.27 f_1 is bounded by the following equation

$$F_1 = 0.0193\,\left|\dot{\theta}\right| + 0.0185\,\dot{\alpha}^2\,\left|cos(\theta)\, sin(\theta)\right| + 2.0534\,\left|cos(\theta)\right| \tag{4.41}$$

Similarly, the maximum value of f_2 corresponds to the maximum values of m_{heli} and l_{cm}

$$\max\{f_2\} = \frac{-B_y\,\dot{\alpha} + 2\,m_{heli\_max}\,l_{cm\_max}^2\,\dot{\alpha}\,\dot{\theta}\,cos(\theta)\,sin(\theta)}{J_y + m_{heli\_max}\,l_{cm\_max}^2\,cos^2(\theta)} \tag{4.42}$$

and the minimum value of f_2 corresponds to the minimum values of m_{heli} and l_{cm}

$$\min\{f_2\} = \frac{-B_y\,\dot{\alpha} + 2\,m_{heli\_min}\,l_{cm\_min}^2\,\dot{\alpha}\,\dot{\theta}\,cos(\theta)\,sin(\theta)}{J_y + m_{heli\_min}\,l_{cm\_min}^2\,cos^2(\theta)} \tag{4.43}$$

The pitch angle is mechanically constrained as $|\theta| \leq 40$. Hence, the maximum and the minimum values of θ are

$$\max\left\{cos^2(\theta)\right\} = cos^2(0) = 1 \tag{4.44}$$

$$\min\left\{cos^2(\theta)\right\} = cos^2(40) = 0.5868 \tag{4.45}$$

The maximum and the minimum values of the $cos^2(\theta)$ and the constants given in Appendix B are used to find a simple expression for $\hat{f}_2$

$$\hat{f}_2 = -12.0378\,\dot{\alpha} + 0.1357\,\dot{\alpha}\,\dot{\theta}\,cos(\theta)\,sin(\theta) \tag{4.46}$$

Equation 3.27 implies that f_2 is bounded by

$$F_2 = 0.3432\;|\dot{\alpha}| + 0.0324\;\left|\dot{\alpha}\,\dot{\theta}\,cos(\theta)\,sin(\theta)\right| \tag{4.47}$$

The maximum and the minimum values of the entries of $\underline{\underline{B}}(\underline{x})$ are the following

$$b_{11\_max} = \frac{K_{pp}}{J_p + m_{heli\_min}\, l_{cm\_min}^2} \tag{4.48}$$

$$b_{12\_max} = \frac{K_{yp}}{J_p + m_{heli\_min}\, l_{cm\_min}^2} \tag{4.49}$$

$$b_{21\_max} = \frac{K_{py}}{J_y + m_{heli\_min}\, l_{cm\_min}^2\, cos^2(\theta)} \tag{4.50}$$

$$b_{22\_max} = \frac{K_{yy}}{J_y + m_{heli\_min}\, l_{cm\_min}^2\, cos^2(\theta)} \tag{4.51}$$

$$b_{11\_min} = \frac{K_{pp}}{J_p + m_{heli\_max}\, l_{cm\_max}^2} \tag{4.52}$$

$$b_{12\_min} = \frac{K_{yp}}{J_p + m_{heli\_max}\, l_{cm\_max}^2} \tag{4.53}$$

$$b_{21\_min} = \frac{K_{py}}{J_y + m_{heli\_max}\, l_{cm\_max}^2\, cos^2(\theta)} \tag{4.54}$$

$$b_{22\_min} = \frac{K_{yy}}{J_y + m_{heli\_max}\, l_{cm\_max}^2\, cos^2(\theta)} \tag{4.55}$$

The entries of the estimated input matrix are obtained by Equation 3.32

$$\hat{b}_{11} = \sqrt{b_{11\_max}\, b_{11\_min}} \tag{4.56}$$

$$\hat{b}_{12} = \sqrt{b_{12\_max}\, b_{12\_min}} \tag{4.57}$$

$$\hat{b}_{21} = \sqrt{b_{21\_max}\, b_{21\_min}} \tag{4.58}$$

$$\hat{b}_{22} = \sqrt{b_{22\_max}\, b_{22\_min}} \tag{4.59}$$

Using Equations 4.48 through 4.59 and the constants given in Appendix B, estimated input matrix is found to be

$$\underline{\underline{\hat{B}}} = \begin{bmatrix} 1.2431 & 0.3621 \\ 0.8108 & 1.5777 \end{bmatrix} \tag{4.60}$$

Since its rows are linearly independent $\underline{\underline{\hat{B}}}$ is invertible. Using Equations 3.33, 3.34, 3.35 and using the maximum and the minimum values for all b_{ij}'s, D_{ii}'s are obtained

$$D_{11} = 0.0154 \tag{4.61}$$

$$D_{22} = 0.0253 \tag{4.62}$$

In this thesis, sliding surfaces are designed as follows

$$\underline{s} = \begin{bmatrix} s_1 \\ s_2 \end{bmatrix} = \begin{bmatrix} \dot{\tilde{x}}_1 + \lambda_{11}\,\tilde{x}_1 + \lambda_{12}\int_0^t \tilde{x}_1\,dr \\ \dot{\tilde{x}}_2 + \lambda_{21}\,\tilde{x}_2 + \lambda_{22}\int_0^t \tilde{x}_2\,dr \end{bmatrix} \tag{4.63}$$

where $\tilde{x}_1 = \theta - \theta_d$, $\tilde{x}_2 = \alpha - \alpha_d$. Positive constants λ_{11}, λ_{12}, λ_{21} and λ_{22} are determined later in this chapter. In order to simplify the calculations $\underline{x}_r$ is defined as follows

$$\underline{\dot{x}}_r = \begin{bmatrix} \dot{x}_{r1} \\ \dot{x}_{r2} \end{bmatrix} = \begin{bmatrix} \dot{x}_1 - s_1 \\ \dot{x}_2 - s_2 \end{bmatrix} \tag{4.64}$$

Since $\underline{\underline{\hat{B}}}$ is found to be invertible, the control law can be given as follows

$$\underline{u} = \underline{\underline{\hat{B}}}^{-1} \left[\underline{\ddot{x}}_r - \underline{\hat{f}}(\underline{x}) - \underline{z}(\underline{s}) \right] \tag{4.65}$$

where

$$\underline{z}(\underline{s}) = \begin{bmatrix} k_1\, sat(s_1/\phi_1) \\ k_2\, sat(s_2/\phi_2) \end{bmatrix} \tag{4.66}$$

ϕ_1 and ϕ_2 are determined at the end of this chapter. Using Equation 3.41 k_1 and k_2 are selected so as to verify sliding conditions.

$$k_1 = \frac{F_1 + D_{11} \max \left\{ \ddot{x}_{r1} - \hat{f}_1 \right\} + \eta_1}{1 - D_{11}} \tag{4.67}$$

$$k_2 = \frac{F_2 + D_{22} \max \left\{ \ddot{x}_{r2} - \hat{f}_2 \right\} + \eta_2}{1 - D_{22}} \tag{4.68}$$

where

$$\max \left\{ \ddot{x}_{r1} - \hat{f}_1 \right\} = \max \left\{ \ddot{x}_{1d} - \lambda_{11}\, \dot{\tilde{x}}_1 - \lambda_{12}\, \tilde{x}_1 - \hat{f}_1 \right\} \tag{4.69}$$

$$= \max \{ \ddot{x}_{1d} \} - \min \{ \lambda_{11}\, \dot{\tilde{x}}_1 \} - \min \{ \lambda_{12}\, \tilde{x}_1 \} - \min \left\{ \hat{f}_1 \right\} \tag{4.70}$$

and

$$\max\left\{\ddot{x}_{r2} - \hat{f}_2\right\} = \max\left\{\ddot{x}_{2d} - \lambda_{21}\,\dot{\tilde{x}}_2 - \lambda_{22}\,\tilde{x}_2 - \hat{f}_2\right\} \tag{4.71}$$

$$= \max\{\ddot{x}_{2d}\} - \min\left\{\lambda_{21}\,\dot{\tilde{x}}_2\right\} - \min\{\lambda_{22}\,\tilde{x}_2\} - \min\left\{\hat{f}_2\right\} \tag{4.72}$$

The maximum values of the $\dot{x}_{1d}$, $\dot{x}_{2d}$, $\ddot{x}_{1d}$ and $\ddot{x}_{2d}$ are calculated from the equations of motions of the system when the input voltages are selected at maximum allowable limits which are 24 and 15 volts for the main and the tail motors respectively. Hence, using the constants given in Appendix B, the following equations are obtained.

$$\ddot{\theta} + 0.9508\,\dot{\theta} + 0.0435\,\dot{\alpha}^2 \leq 34.1896\,rad/s^2 \tag{4.73}$$

$$\ddot{\alpha} + 13.5686\,\dot{\alpha} - 0.0920\,\dot{\alpha}\,\dot{\theta} \leq 43.4863\,rad/s^2 \tag{4.74}$$

$\min\{cos(\theta)\} = cos(40) = 0.766$ is used for the first and $\max\{cos(\theta)\} = cos(0) = 1$ is used for the second equation to get the maximum values of the right hand side of the equations above. Bounds of the first and the second derivatives of the pitch and yaw angles can be chosen as follows

$$\left|\dot{\theta}\right| \leq 1\,rad/s^2 \qquad |\dot{\alpha}| \leq 1\,rad/s^2 \qquad \left|\ddot{\theta}\right| \leq 2\,rad/s^2 \qquad |\ddot{\alpha}| \leq 2\,rad/s^2 \tag{4.75}$$

The derivatives of the desired values can be chosen to be bounded by these equations. In Equations 4.70 and 4.72, the difference between the derivative of the actual and the desired pitch and yaw angles can be taken as the bounds of these values.

$$\min\left\{\lambda_{11}\,\dot{\tilde{x}}_1\right\} = -\lambda_1 \tag{4.76}$$

$$\min\left\{\lambda_{21}\,\dot{\tilde{x}}_2\right\} = -\lambda_2 \tag{4.77}$$

In Equations 4.70 and 4.72, $\tilde{x}_1$ and $\tilde{x}_2$ can be taken as zero. The minimum value of $\hat{f}_1$ is obtained from Equation 4.40 when $\max\{cos(\theta)\} = cos(0) = 1$ and $\max\left\{\dot{\theta}\right\} = 1$

$$\min\left\{\hat{f}_1\right\} = -16.6298\,rad/s^2 \tag{4.78}$$

The minimum value of $\hat{f}_2$ is obtained from Equation 4.46 when $\max\{sin(\theta)\,cos(\theta)\} = sin(40)\,cos(40) = 0.4924$, $\max\{\dot{\alpha}\} = 1$ and $\max\left\{\dot{\theta}\right\} = 1$

$$\min\left\{\hat{f}_2\right\} = -11.97\,rad/s^2 \tag{4.79}$$

Substituting Equations 4.75, 4.76 and 4.78 into Equation 4.67 and substituting Equations 4.75, 4.77 and 4.79 into Equation 4.68 lead to

$$k_1 = \frac{F_1 + D_{11}\,(18.6298 + \lambda_1) + \eta_1}{1 - D_{11}} \tag{4.80}$$

$$k_2 = \frac{F_2 + D_{22}\,(13.97 + \lambda_2) + \eta_2}{1 - D_{22}} \tag{4.81}$$

η_1 and η_2 determines the size of the control inputs outside the surfaces and are chosen after numerous trials

$$\eta_1 = 0.2 \qquad \eta_2 = 1.5 \tag{4.82}$$

ϕ_1 and ϕ_2 are proportional to the steady-state error whereas λ_1 and λ_2 are in inverse proportion to the steady-state error. These constants are related with each other and determined by trial and error.

$$\phi_1 = 0.5 \qquad \phi_2 = 0.1 \tag{4.83}$$

$$\lambda_{11} = 10 \qquad \lambda_{21} = 12 \tag{4.84}$$

$$\lambda_{12} = 1.2 \qquad \lambda_{22} = 0.2 \tag{4.85}$$

5. EXPERIMENTAL RESULTS

Controllers that are designed according to the various methodologies are implemented in the Simulink tool of MATLAB software.

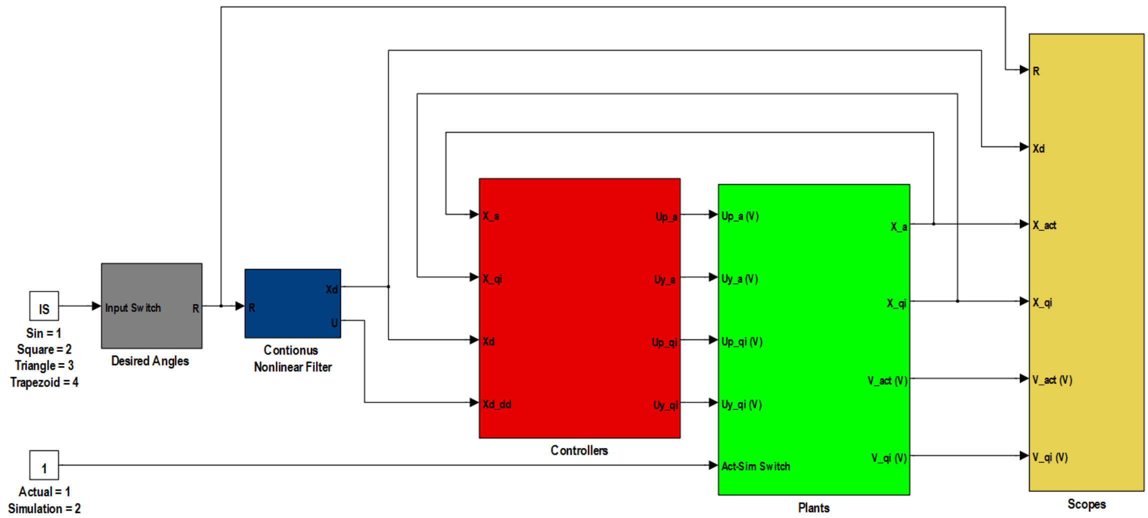

Figure 5.1. Overview in Simulink environment.

The nonlinear model of the system is used in simulation and the results of the model is compared with the physical system in various scenarios. Different reference trajectories are tracked with nominal and loaded helicopter system. The first four scenarios compare the feedback linearization controller and sliding mode controller when they don't have integral action. In the last two scenarios, integral action is used in the all controllers, namely full-state feedback controller, the feedback linearization controller and the sliding mode controller and they are compared with each other. In addition, the reference pitch and the yaw angles, the output of the filter and the outputs of the simulated and the physical system are plotted on the same graph. Moreover, control inputs of the motors are also represented in the following graphs. In these graphs, blue line represents the reference signal, red line shows the output of continous nonlinear filter, measured signal is indicated by black line and the output of simulation is shown by magenta line.

- Scenario 1

  In this experiment, nominal helicopter model is used. The sinusoidal wave with a magnitude of 10 degrees is the reference input for the pitch angle and zero reference is tracked by the yaw angle.

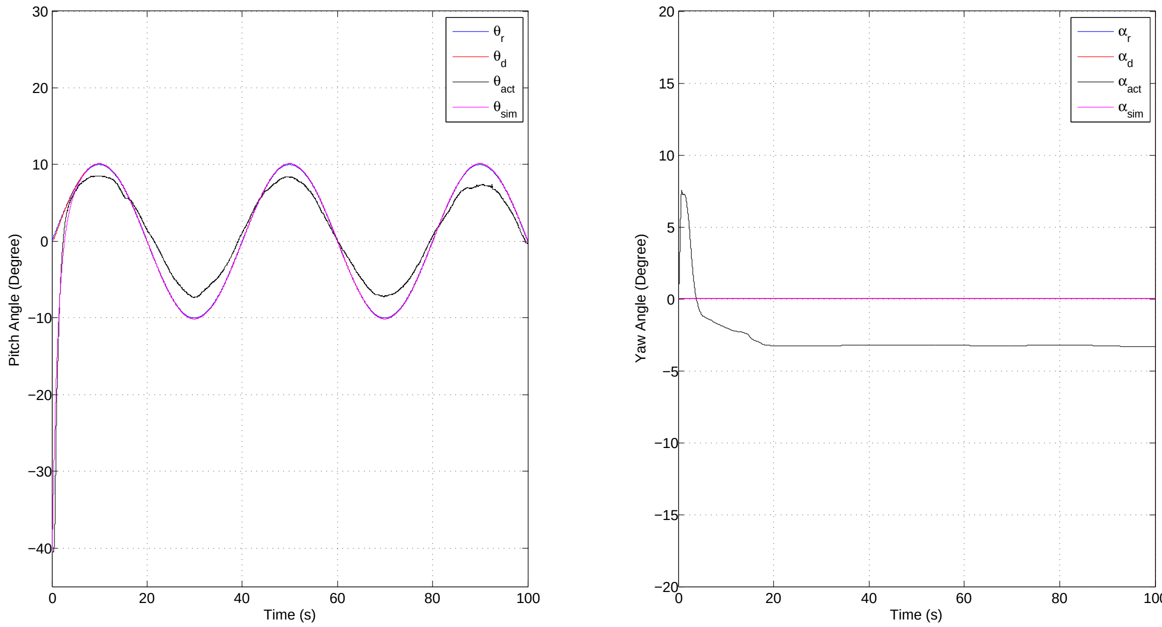

Figure 5.2. Outputs of the simulated and the physical system for FL controller.

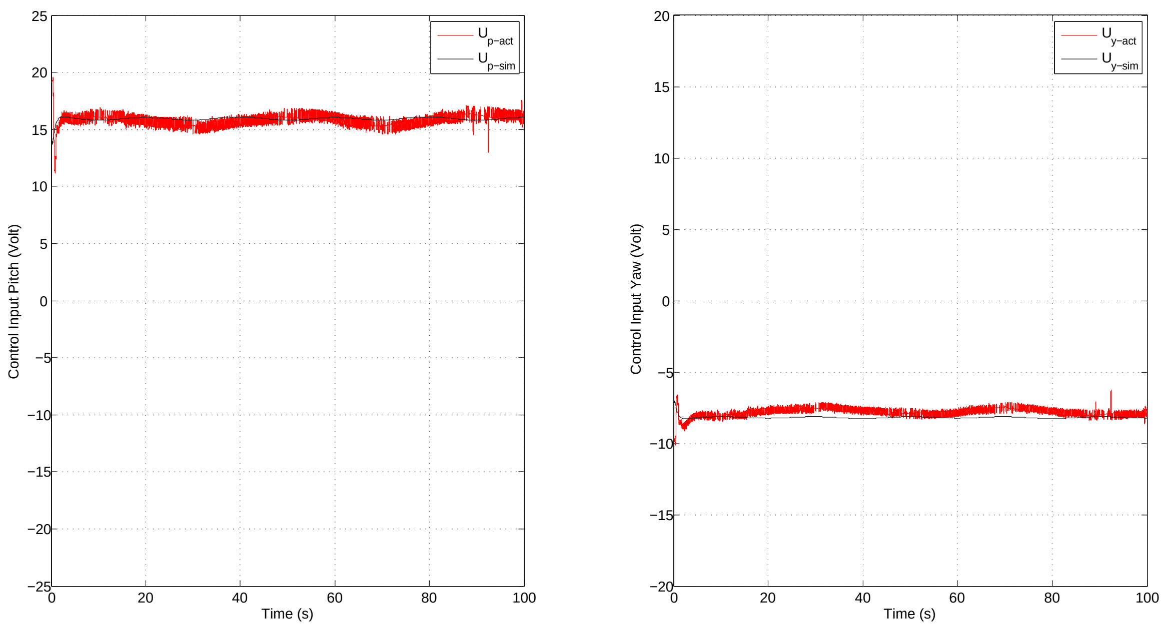

Figure 5.3. Control inputs of the simulated and the physical system for FL controller.

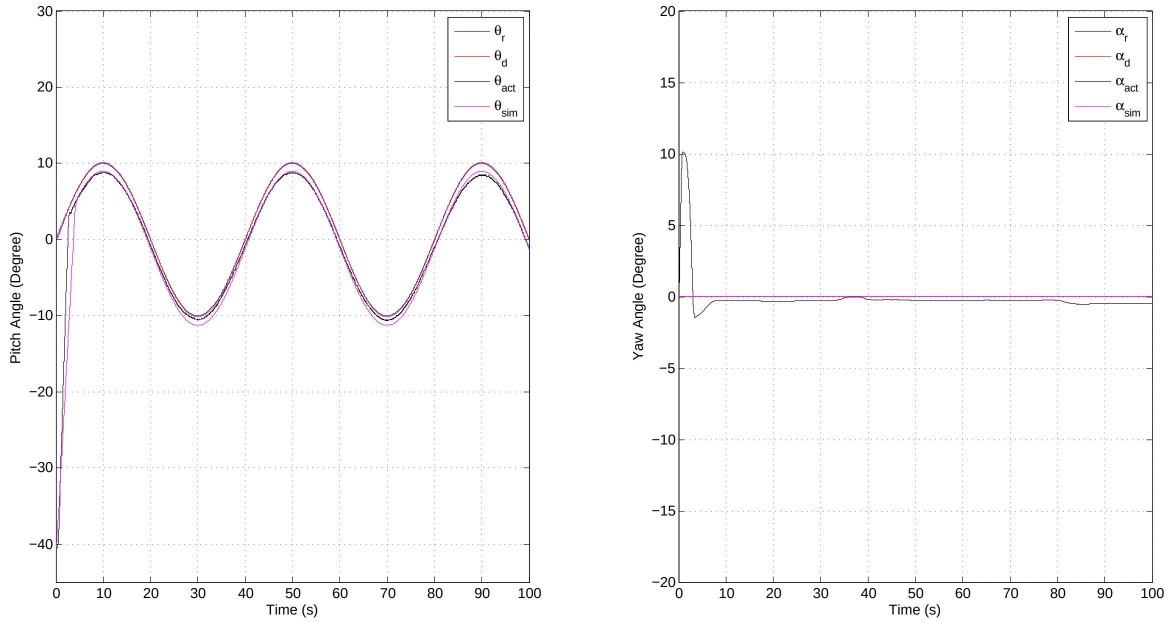

Figure 5.4. Outputs of the simulated and the physical system for SMC controller.

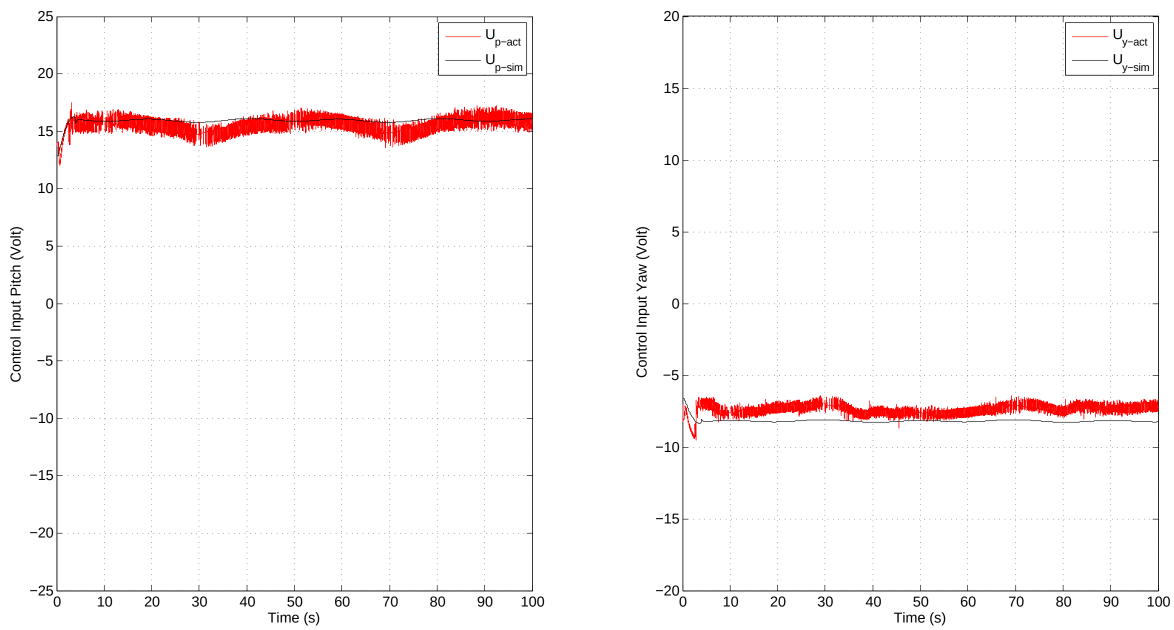

Figure 5.5. Control inputs of the simulated and the physical system for SMC controller.

In simulation results, the feedback linearization controller yields zero steady-state error for both pitch and yaw angles because it is designed according to the nonlinear mathematical model of the system which is used in the simulation. The feedback linearization controller has no overshoot and better settling time as compared to the sliding mode controller. The sliding mode controller has a constant boundary layer thickness; therefore, the system trajectories do not converge to the sliding surfaces, but they stay close to it. Hence, the sliding mode controller has some steady-state error for the pitch angle and almost zero steady-state error for yaw angle because the boundary layer thickness of the surface associated with the pitch axis is more than the yaw axis's boundary layer thickness.

In the experiment, the sliding mode controller which deals with modeling uncertainties provides better steady-state error than the feedback linearization controller for both pitch and yaw angles. The sliding mode controller has satisfactory settling time and no overshoot for the pitch angle. On the other hand, it has greater overshoot than the feedback linearization controller for the yaw angle. However, steady state error of the sliding mode controller is lower than the feedback linearization controller's and almost zero. Moreover, control input of the sliding mode controller is more oscillatory than the control input of the feedback linearization controller for both motors.

- Scenario 2

  In this experiment, nominal helicopter model is used. The square wave with a magnitude of 10 degrees is the reference input for the pitch angle and zero reference is tracked by the yaw angle.

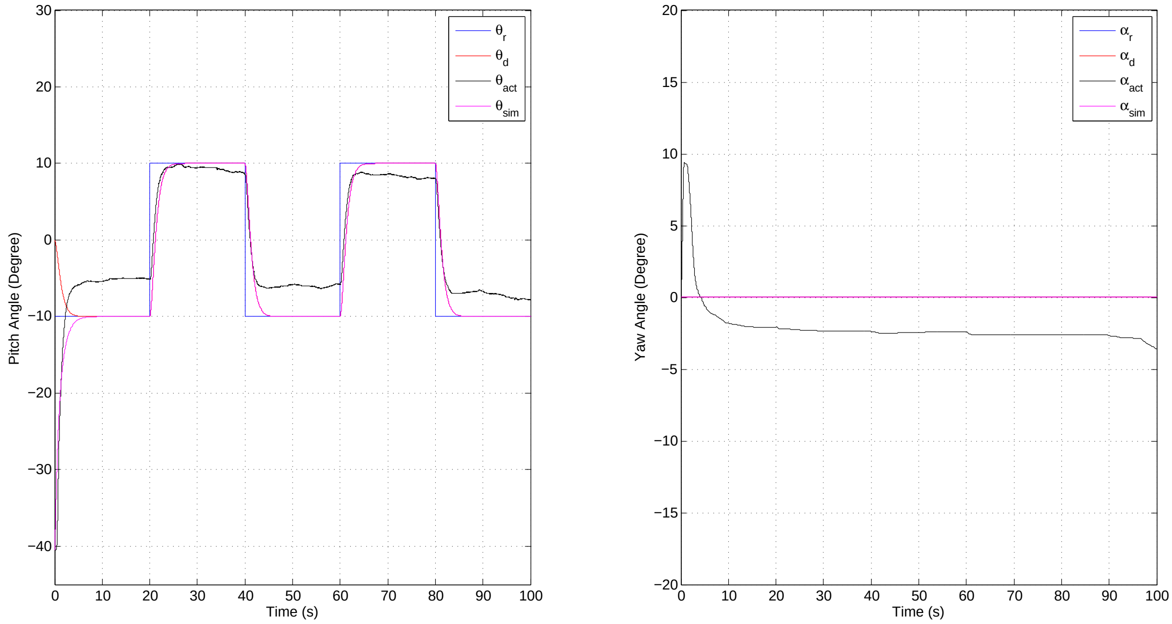

Figure 5.6. Outputs of the simulated and the physical system for FL controller.

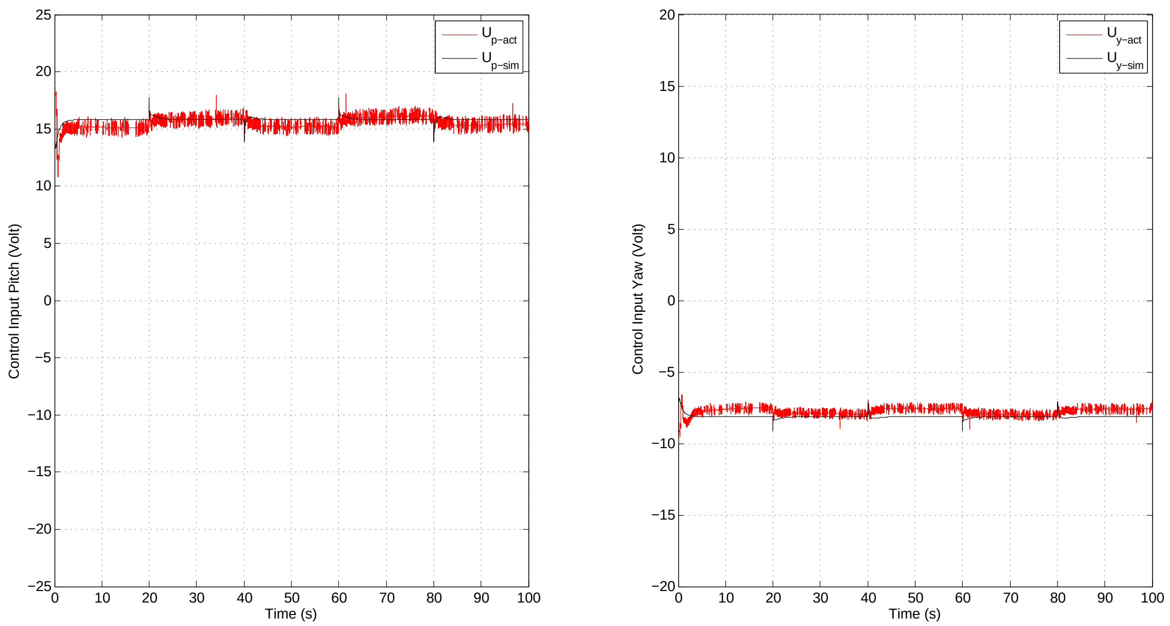

Figure 5.7. Control inputs of the simulated and the physical system for FL controller.

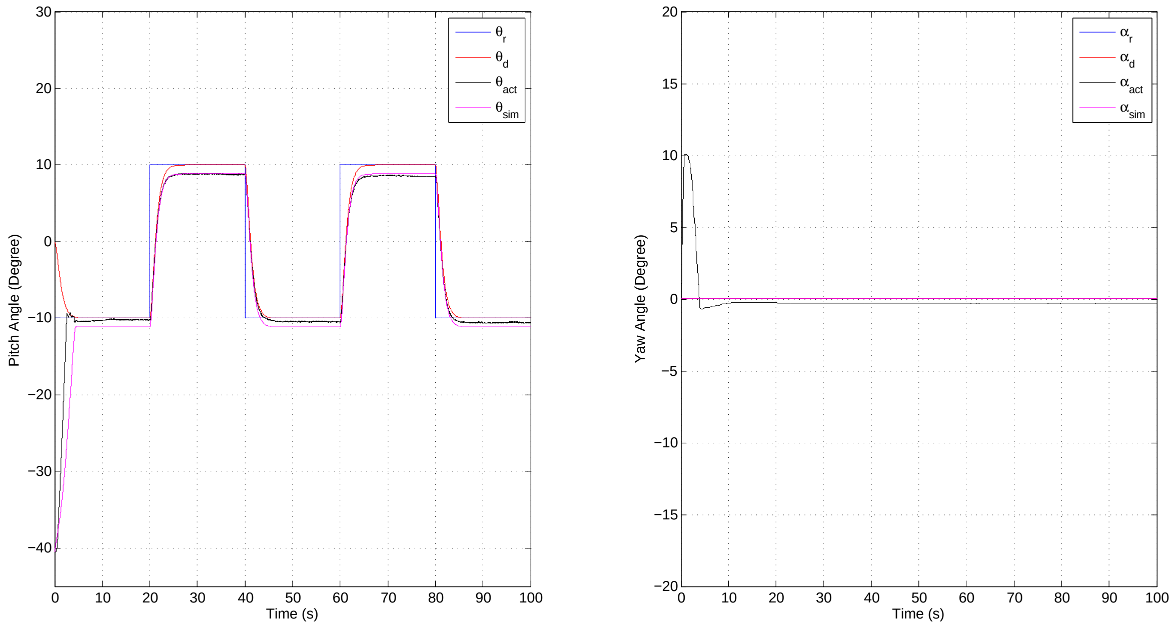

Figure 5.8. Outputs of the simulated and the physical system for SMC controller.

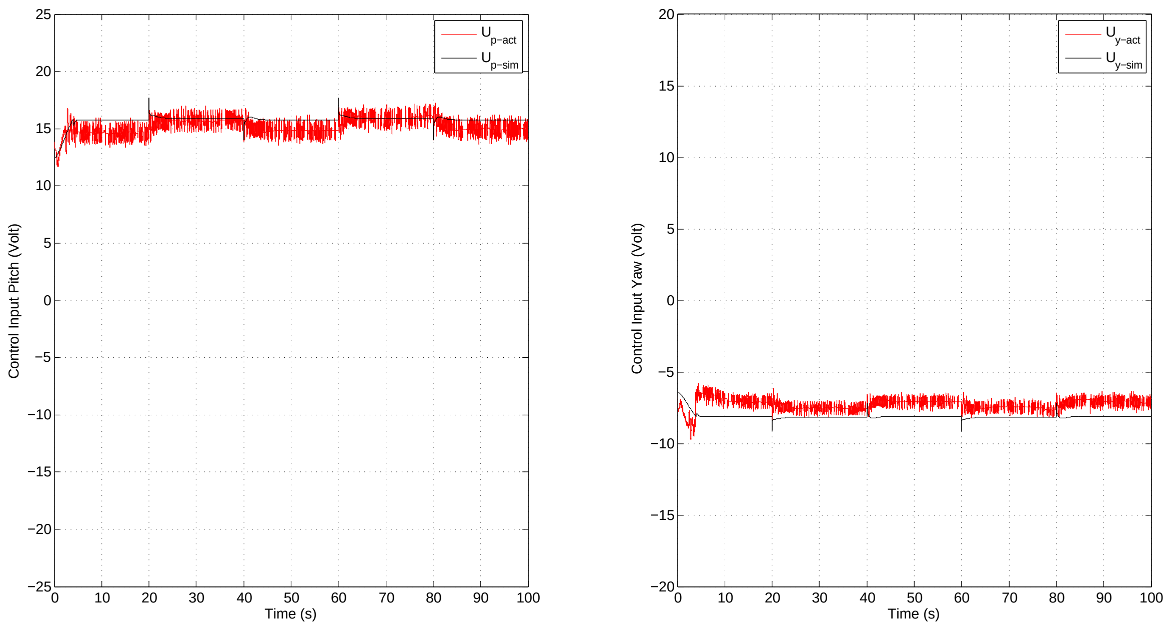

Figure 5.9. Control inputs of the simulated and the physical system for SMC controller.

Same results are obtained for simulation as in the first scenario. The feedback linearization controller yields zero steady-state error for both pitch and yaw angles. This controller has no overshoot and better settling time as compared to the sliding mode controller. The sliding mode controller has some steady-state error for the pitch angle and almost zero steady-state error for yaw angle.

In the experiment, the sliding mode controller provides better steady-state error than the feedback linearization controller for both pitch and yaw angles. The sliding mode controller has satisfactory settling time and no overshoot for the pitch angle. On the other hand, it has slightly greater overshoot than the feedback linearization controller for the yaw angle. However, steady-state error of the sliding mode controller is less than the feedback linearization controller's and almost zero. Moreover, the sliding mode controller has more oscillatory control input than the feedback linearization controller for both motors.

- Scenario 3

  In this experiment, additional load is mounted on the body of the helicopter. The sinusoidal wave with a magnitude of 10 degrees is the reference input for the pitch angle and zero reference is tracked by the yaw angle.

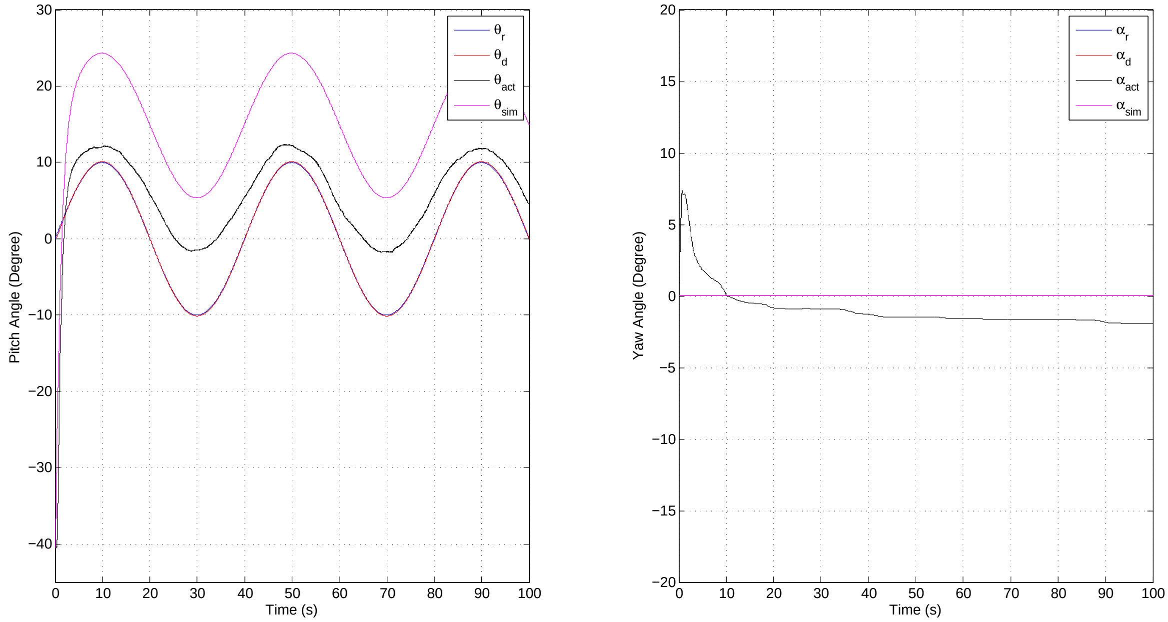

Figure 5.10. Outputs of the simulated and the physical system for FL controller.

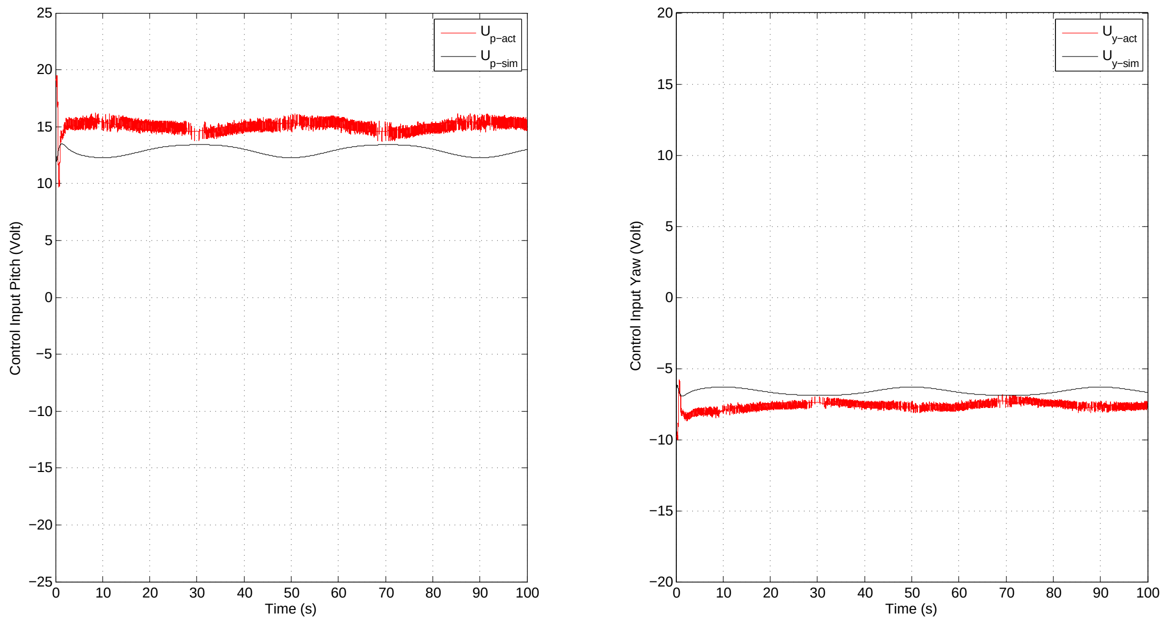

Figure 5.11. Control inputs of the simulated and the physical system for FL controller.

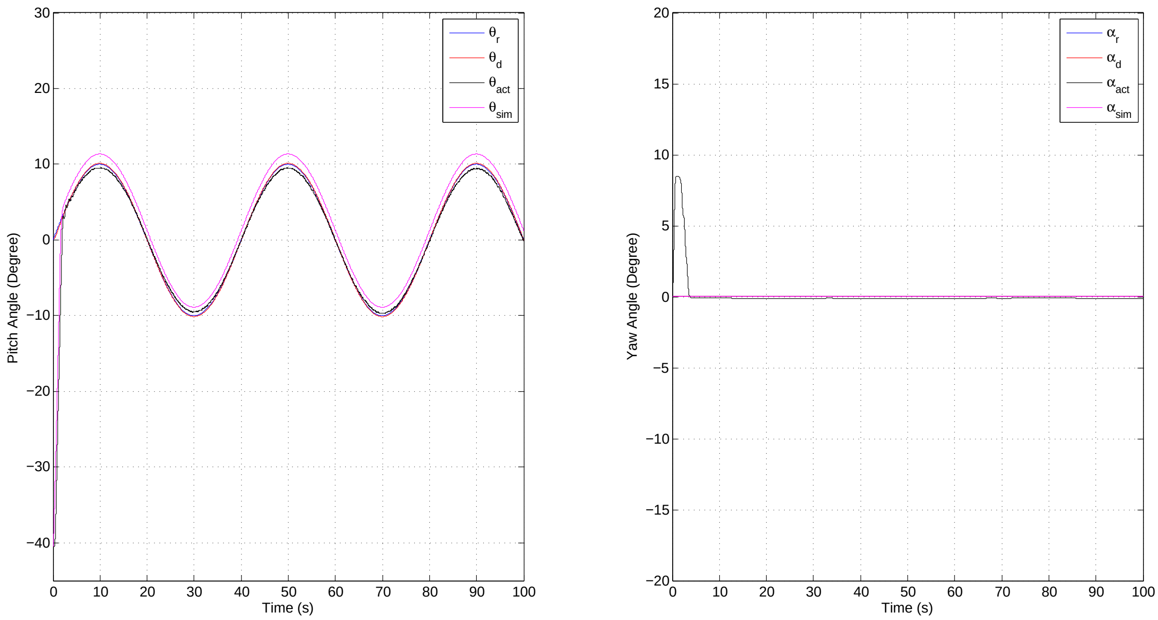

Figure 5.12. Outputs of the simulated and the physical system for SMC controller.

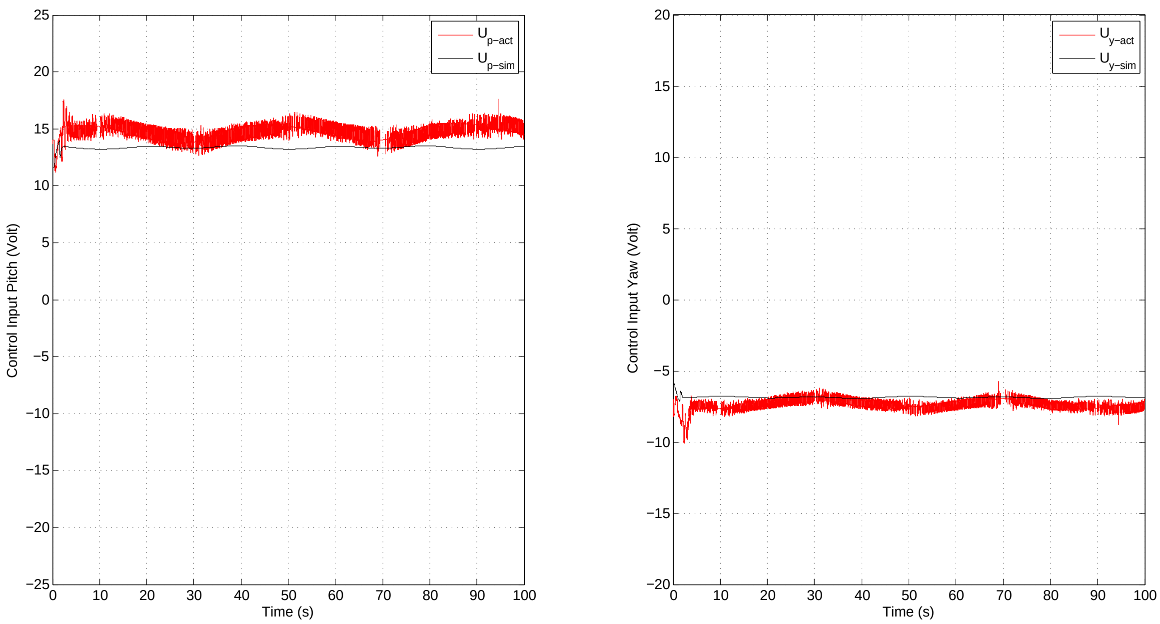

Figure 5.13. Control inputs of the simulated and the physical system for SMC controller.

In simulation results, the sliding mode controller and the feedback linearization controller have zero steady-state errors for the yaw angle. However, the sliding mode controller provides significantly better steady-state error than the feedback linearization controller for pitch angle because of its robustness to parameter changes. Control input of the sliding mode controller has lower peak value than the control input of the feedback linearization controller for the main motor which is acting on pitch axis.

In the experiment, the sliding mode controller provides considerably better steady-state error than the feedback linearization controller for both pitch and yaw angles while having more oscillatory control input than the feedback linearization controller for both motors.

- Scenario 4

  In this experiment, additional load is mounted on the body of the helicopter. The square wave with a magnitude of 10 degrees is the reference input for the pitch angle and zero reference is tracked by the yaw angle.

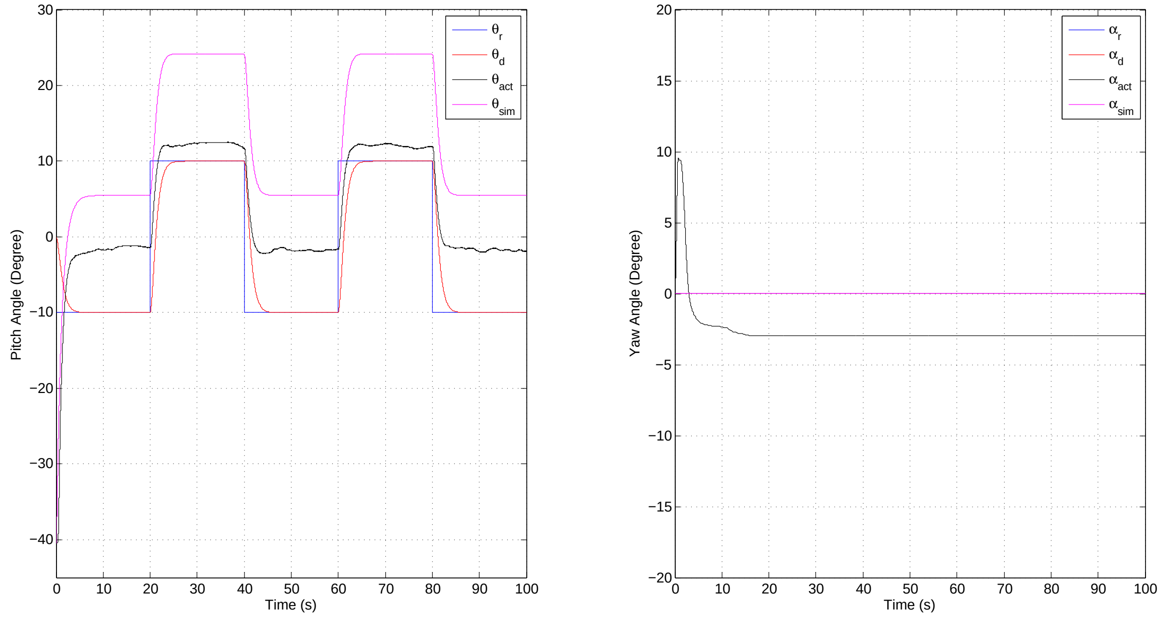

Figure 5.14. Outputs of the simulated and the physical system for FL controller.

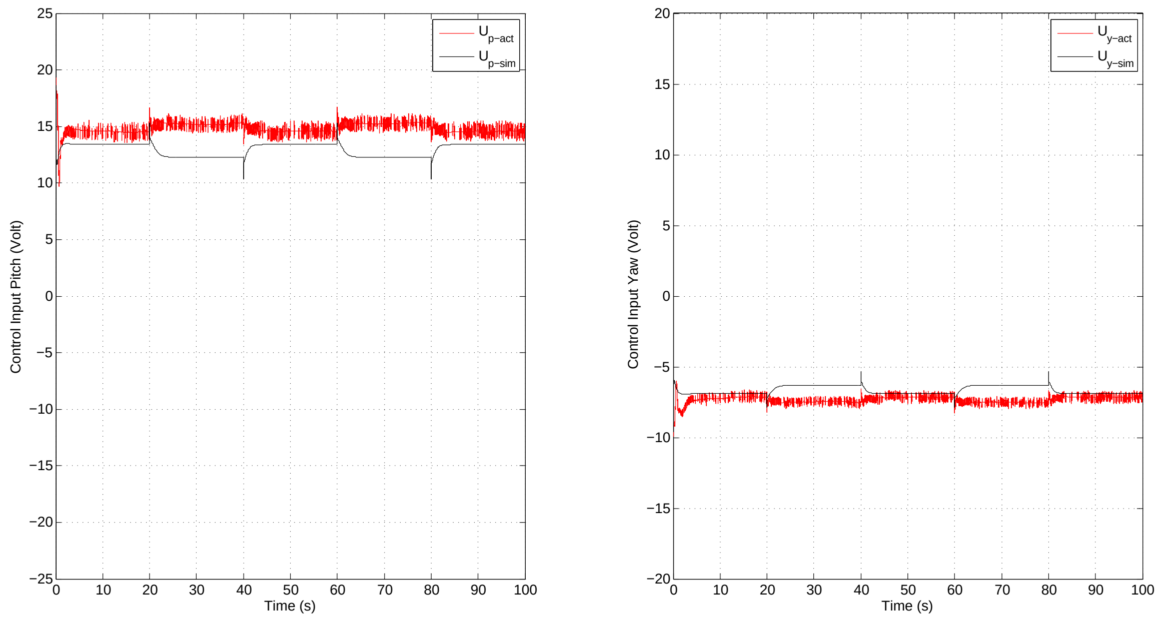

Figure 5.15. Control inputs of the simulated and the physical system for FL controller.

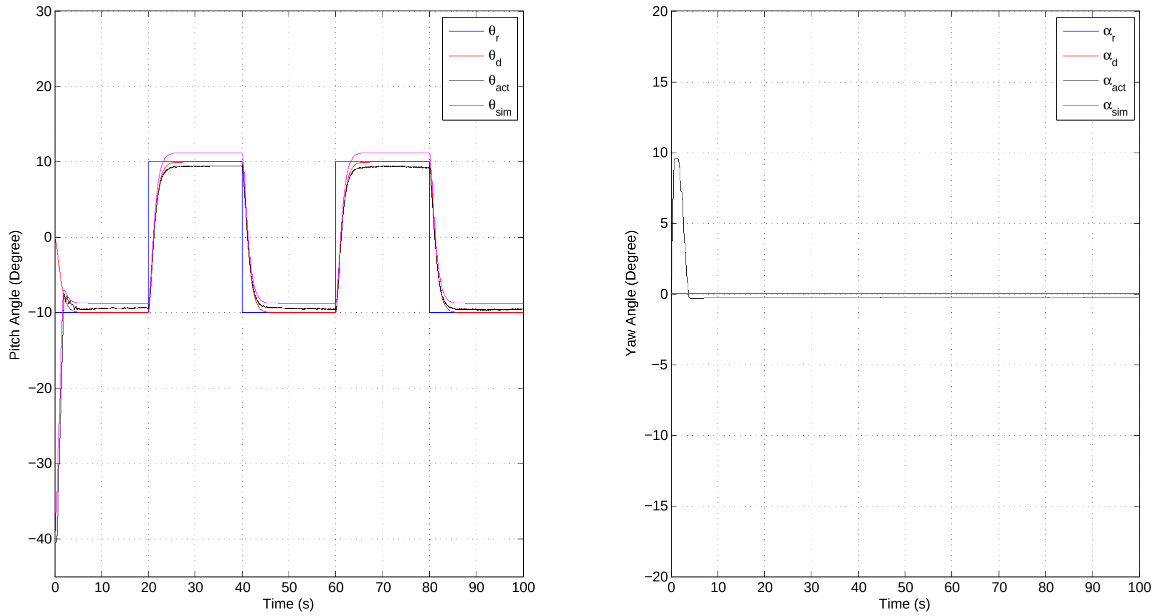

Figure 5.16. Outputs of the simulated and the physical system for SMC controller.

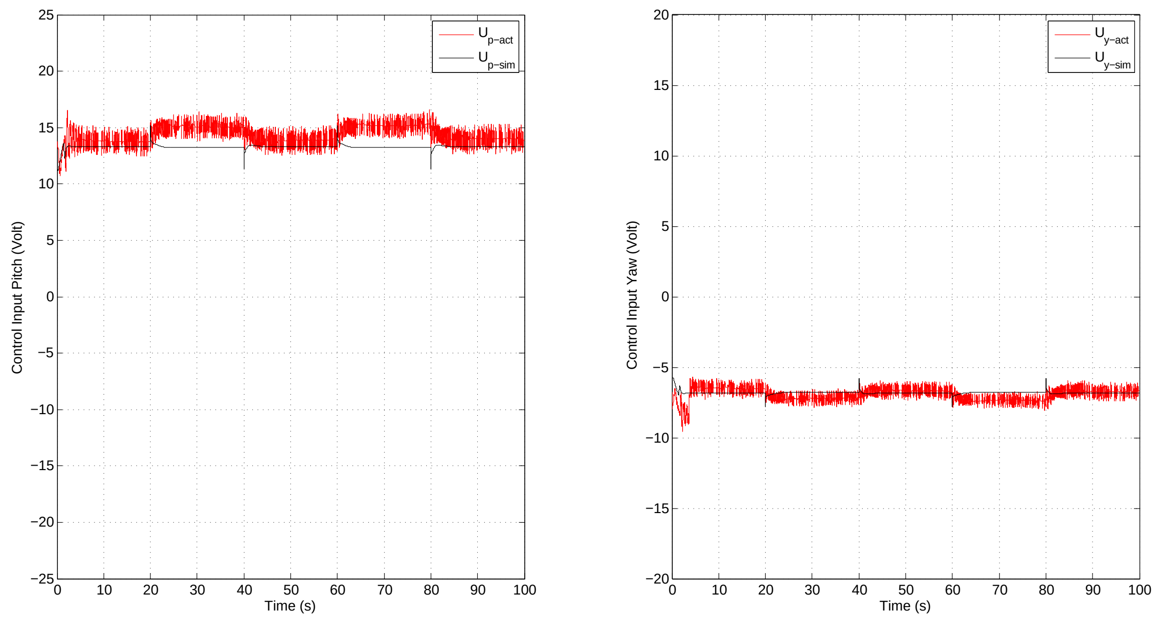

Figure 5.17. Control inputs of the simulated and the physical system for SMC controller.

In simulation results, the sliding mode controller and the feedback linearization controller have zero steady-state errors for yaw angle but the former yields considerably better steady-state error for the pitch angle than the latter one.

In the experiment, sliding mode controller provides considerably better steady-state error than the feedback linearization controller for both pitch and yaw angles while having more oscillatory control input than the feedback linearization controller for both motors.

- Scenario 5

  In this experiment, nominal helicopter model is used. The square wave with a magnitude of 10 degrees is the reference input for the pitch angle and zero reference is tracked by the yaw angle. This time, however, integral action is used in the controllers.

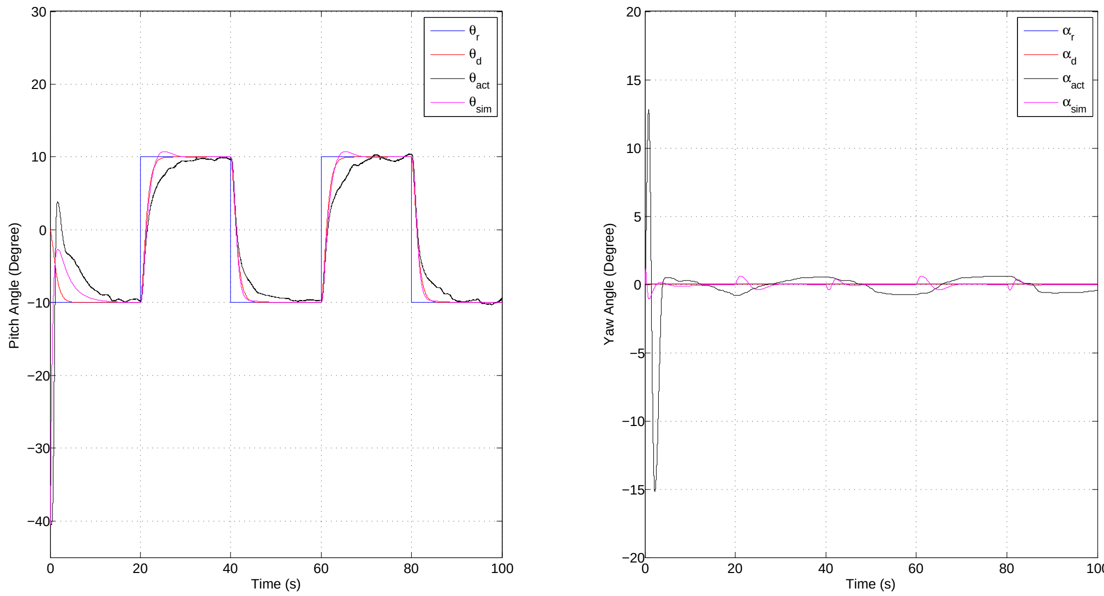

Figure 5.18. Outputs of the simulated and the physical system for FSFC controller with integral action.

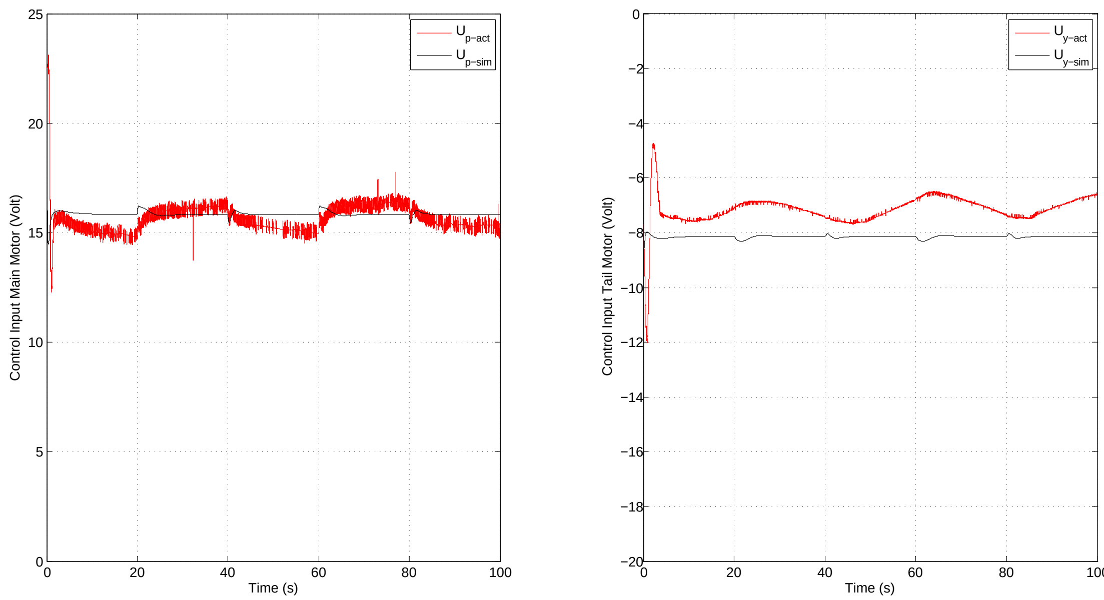

Figure 5.19. Control inputs of the simulated and the physical system for FSFC controller with integral action.

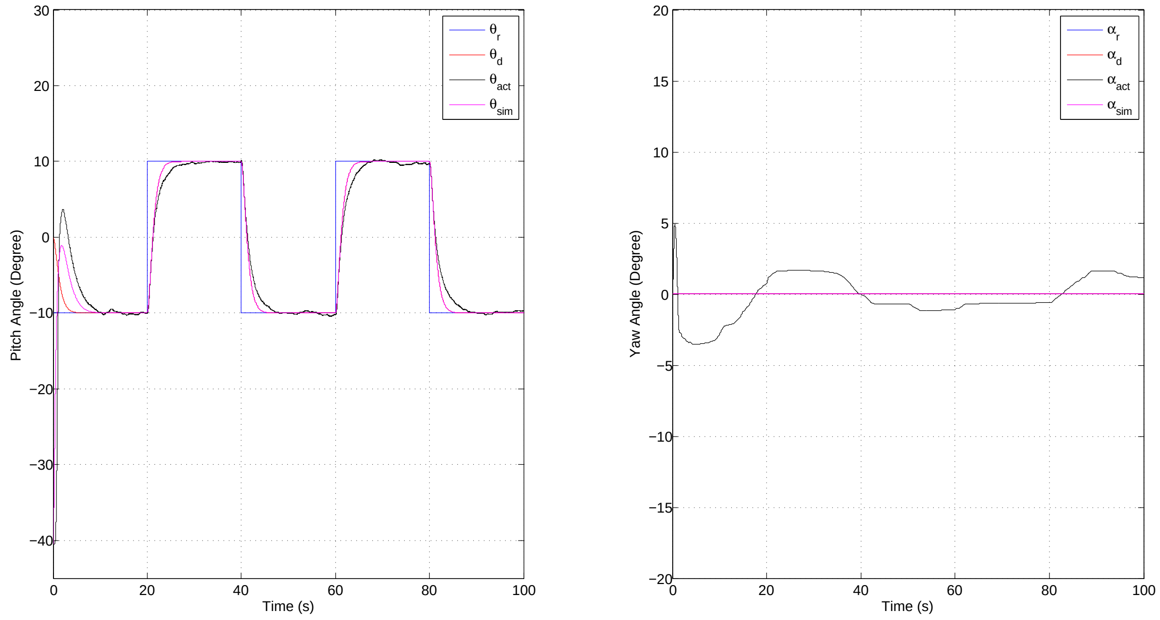

Figure 5.20. Outputs of the simulated and the physical system for FL controller with integral action.

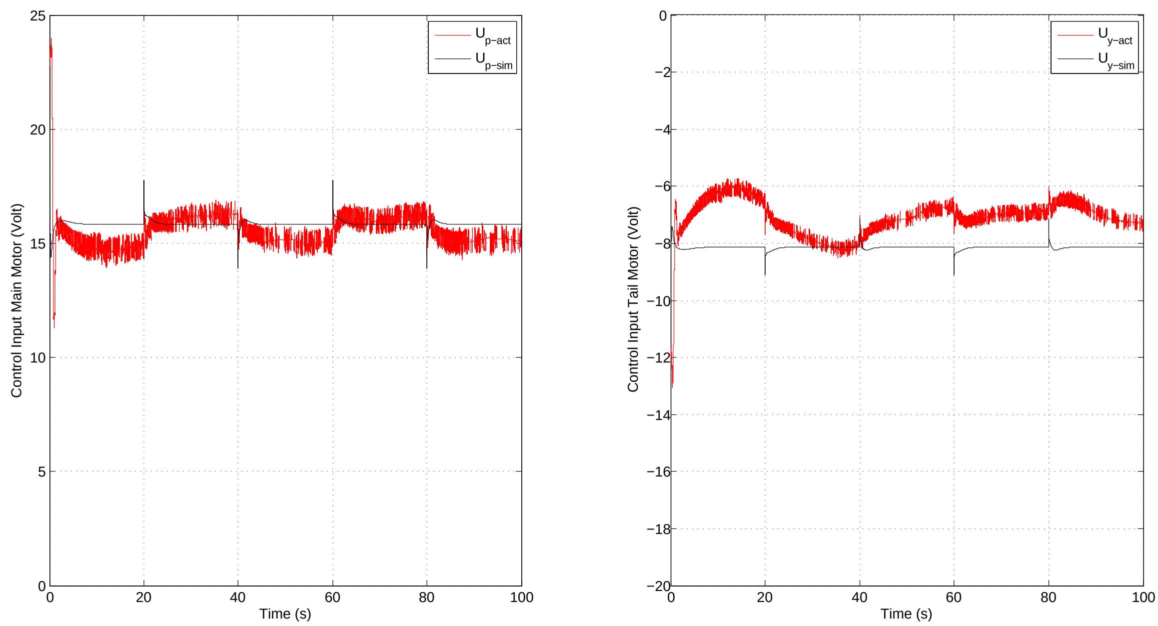

Figure 5.21. Control inputs of the simulated and the physical system for FL controller with integral action.

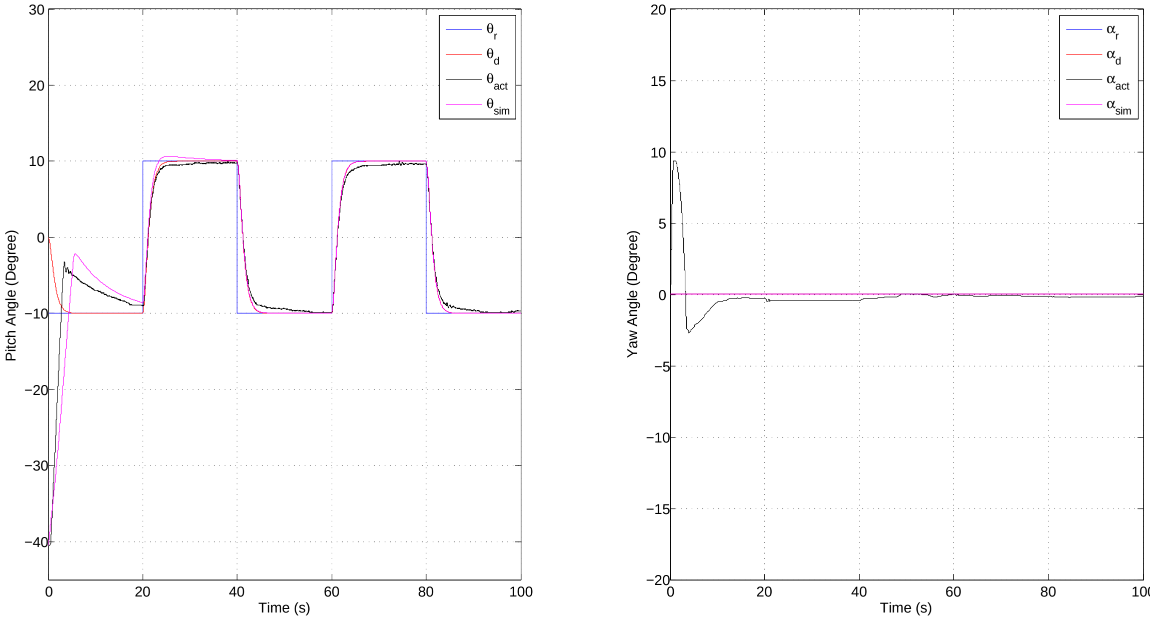

Figure 5.22. Outputs of the simulated and the physical system for SMC controller with integral action.

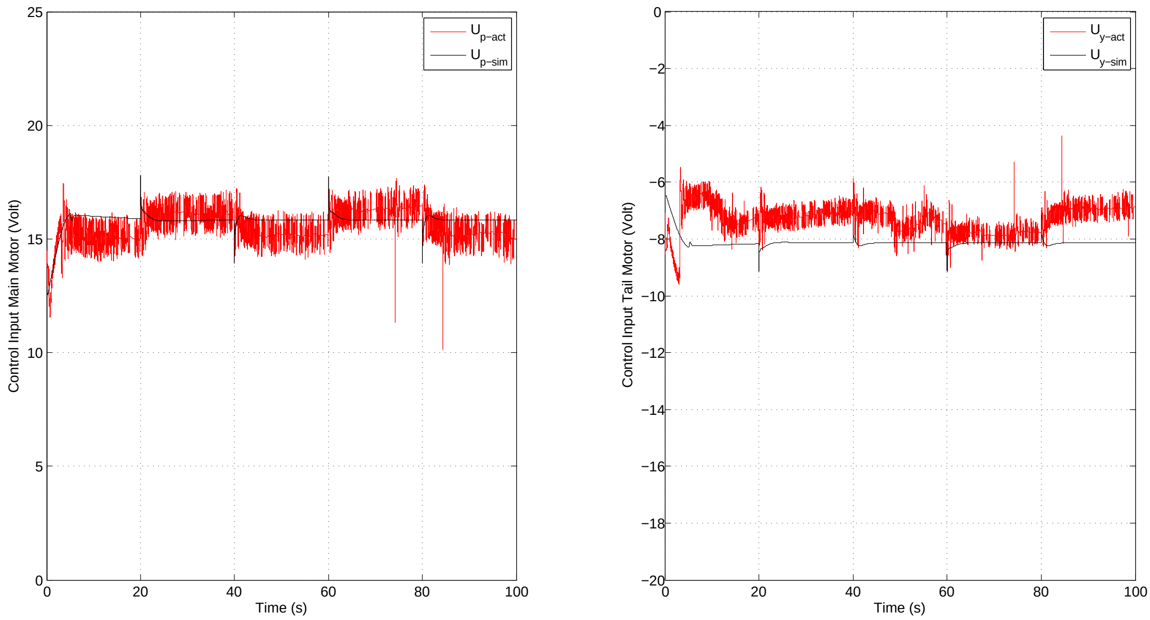

Figure 5.23. Control inputs of the simulated and the physical system for SMC controller with integral action.

In simulation results, all the controllers have almost the same overshoot and settling time for the pitch angle. In addition, these controllers have zero steady-state error thanks to the integrators. Although the sliding mode controller has less overshoot than the feedback linearization controller, it has greater settling time than the feedback linearization controller. Because of the inaccuraties of some parameters in mathematical model, the full-state feedback controller and the feedback linearization controller have some steady-state error for yaw angle as shown in the figures 5.18 and 5.20. However, the sliding mode controller have zero steady-state error since it is robust against the inaccuraties of the mathematical model.

In the experiment, the full-state feedback controller have a little steady-state error on the pitch and yaw angle because it has a control input which includes a feedforward term that depends on mathematical model of the system. Because of the inaccuraties of some parameters in mathematical model, the feedback linearization controller have steady-state error. However, it has zero steady-state error for the yaw angle. The sliding mode controller has zero steady-state error for both angles. It has less overshoot than the other controllers for the pitch angle but the settling time of the sliding mode controller is greater than the feedback linearization controller's for the same angle. Moreover, overshoot of the sliding mode controller is less than the overshoot of the full-state feedback controller and greater than the overshoot of the feedback linearization controller. Finally, control input of the sliding mode controller is more oscillatory than the other controllers'.

- Scenario 6

  In this experiment, additional load is mounted on the body of the helicopter. The square wave with a magnitude of 10 degrees is the reference input for the pitch angle and zero reference is tracked by the yaw angle.

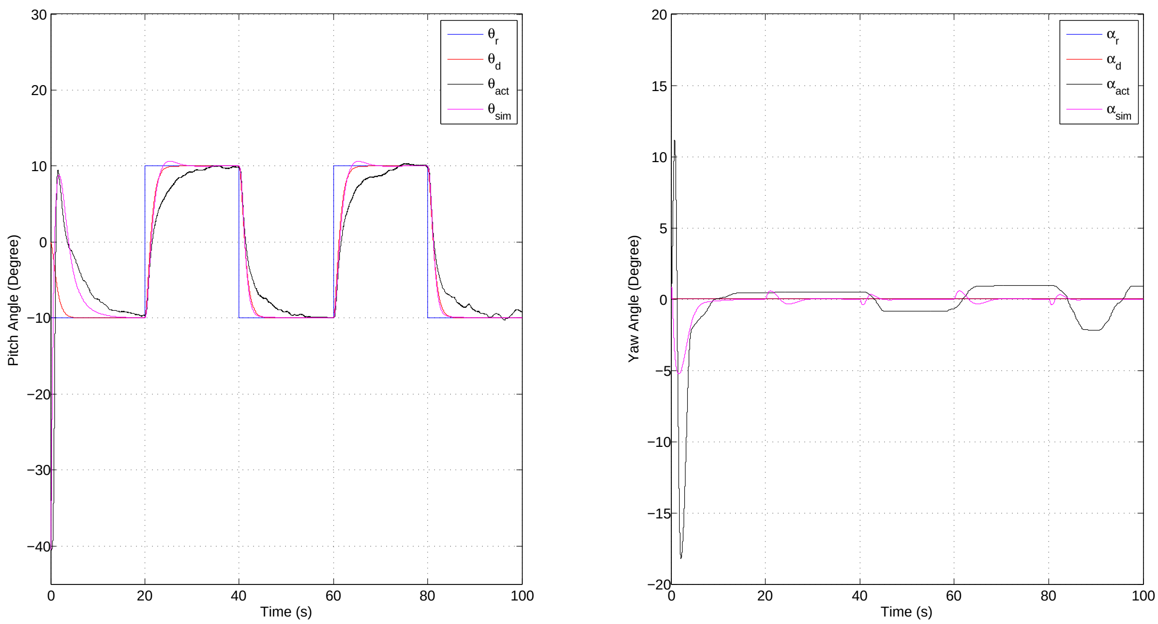

Figure 5.24. Outputs of the simulated and the physical system for FSFC controller with integral action.

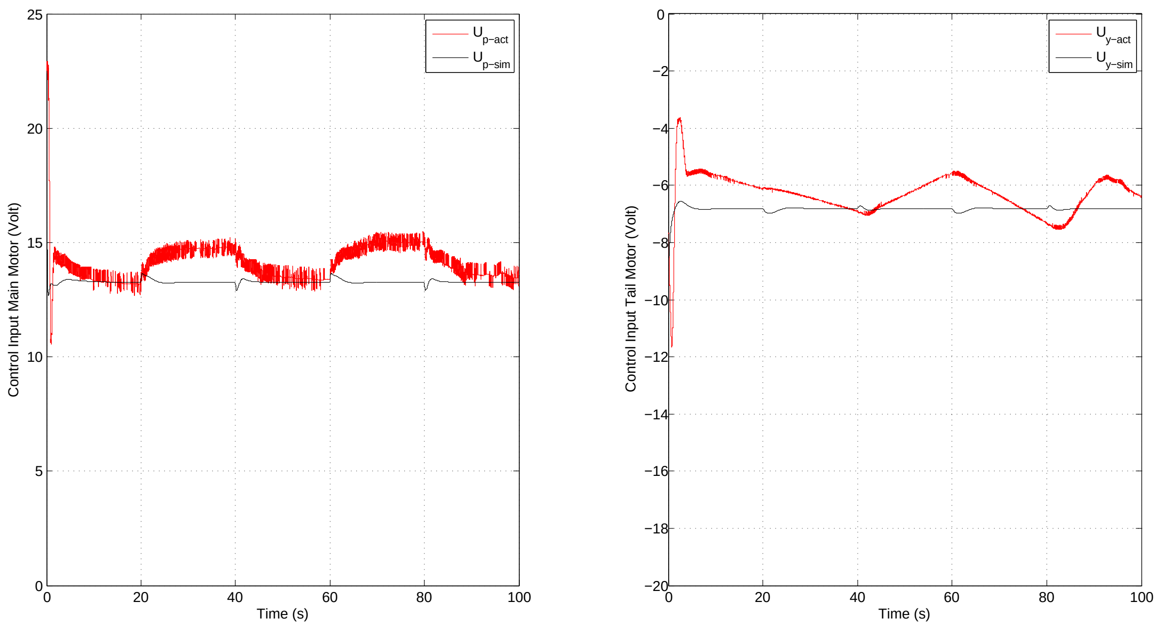

Figure 5.25. Control inputs of the simulated and the physical system for FSFC controller with integral action.

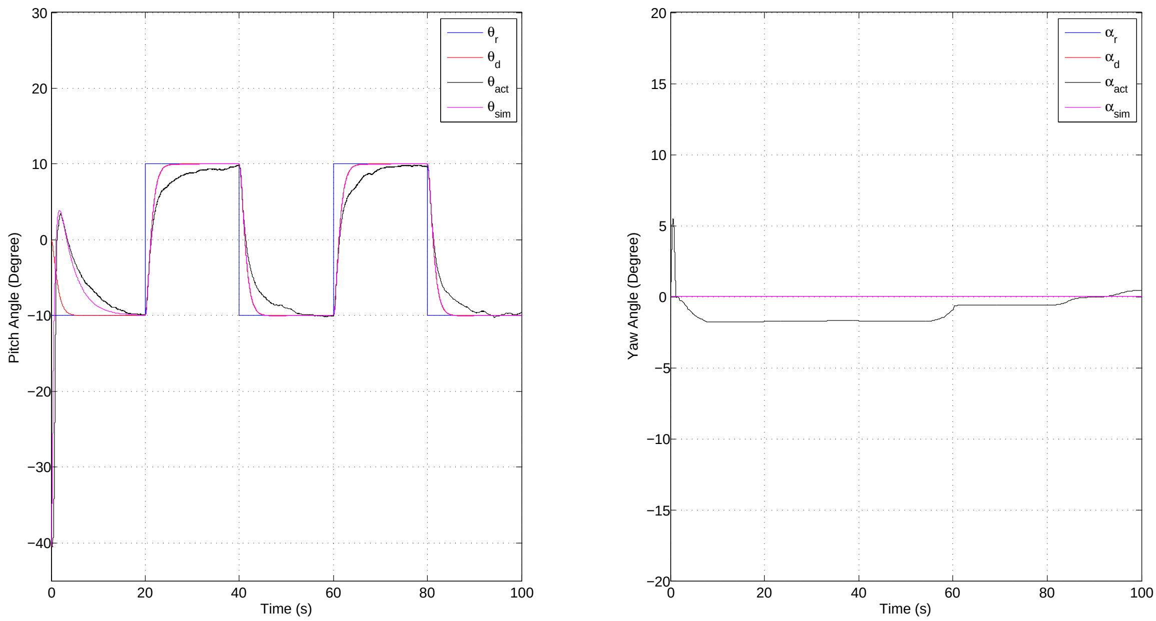

Figure 5.26. Outputs of the simulated and the physical system for FL controller with integral action.

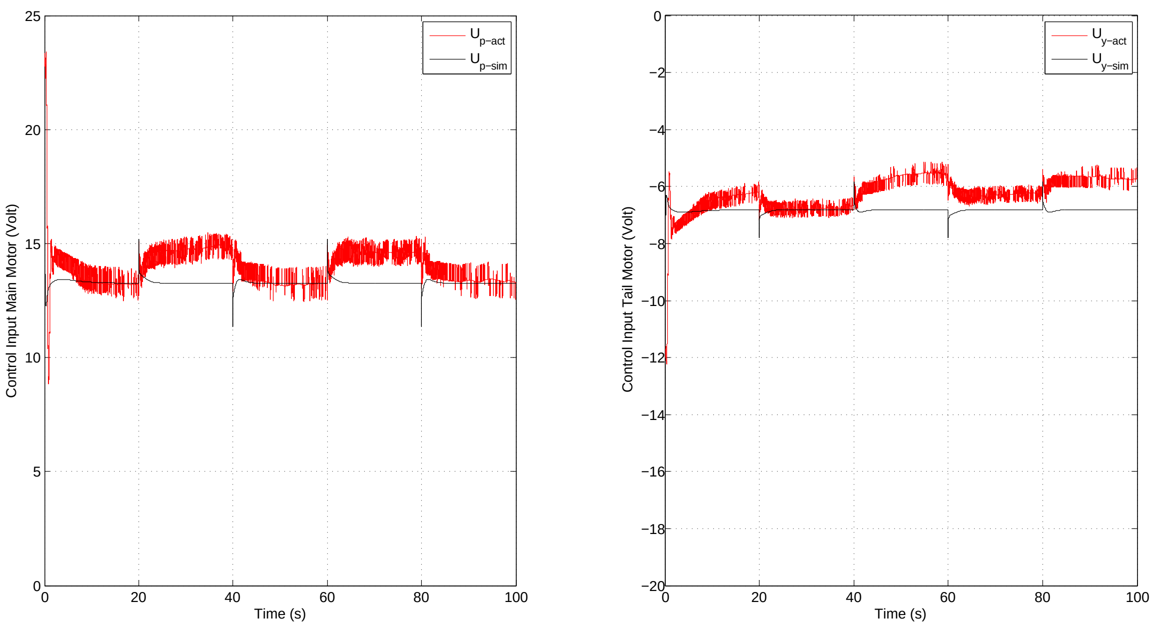

Figure 5.27. Control inputs of the simulated and the physical system for FL controller with integral action.

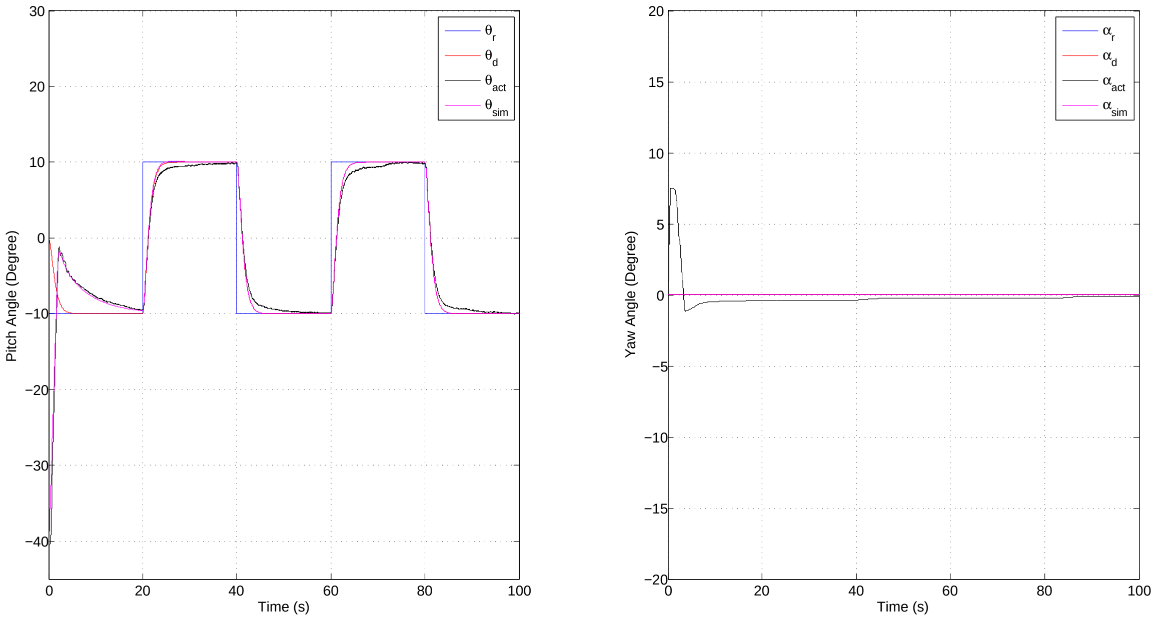

Figure 5.28. Outputs of the simulated and the physical system for SMC controller with integral action.

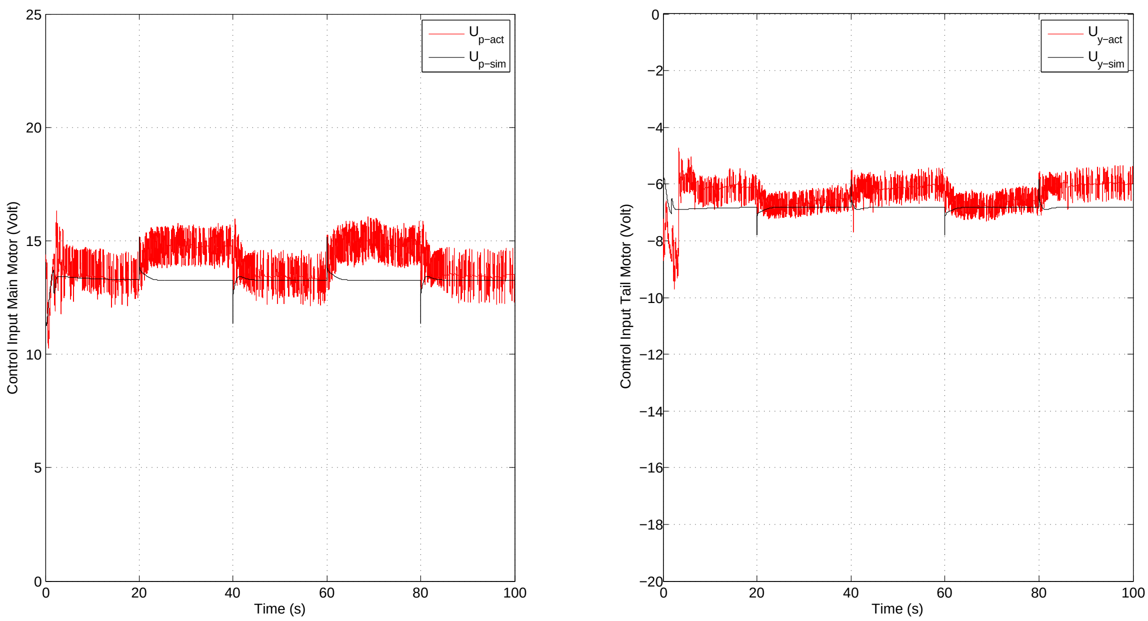

Figure 5.29. Control inputs of the simulated and the physical system for SMC controller with integral action.

In simulation results, all the controllers have zero steady-state error for the pitch and yaw angles. The overshoot of the sliding mode controller is less than the overshoot of the other controllers' for the pitch angle. On the other hand, it has greater settling time than the other controllers'.

In the experiment, all the controllers have zero steady-state error for the pitch angle. This time, however, the sliding mode controller provides better settling time and overshoot than the other controllers for the pitch angle. The overshoot of the sliding mode controller is greater than the overshoot of the feedback linearization controller for the yaw angle. However, the sliding mode controller provides zero steady-state error.

6. CONCLUSION

In this thesis, the mathematical model of the system is derived and critical parameters of the model are calibrated. The nonlinear equations of motions with improved parameters are used to design the sliding mode and feedback linearization controllers. On the other hand, full-state feedback controller is based on locally linearized equations. In simulation results, the feedback linearization controller performed slightly better then the sliding mode controller in the first and the second scenarios because they were applied to the nominal system. When, however, additional load is put on the helicopter in order to create a deviation from the nominal model, the sliding mode controller yields significantly better results than the feedback linearization controller. After using integral action in the controllers, the difference between the performances of the controllers reduced. However, as expected, performance of the sliding mode controller was better than the other controllers, in the fifth and sixth scenarios.

Although the overall performance of the sliding mode controller seems to be the best one among the others', it suffers under the typical chattering problem that needs to be improved in future studies. Chattering problem can be handled with increasing the boundary layer thickness of the surfaces. However, this action raises the steady-state error. Because of this trade-off between boundary layer thickness and steady-state error, the selection of the boundary layer thickness is based on the experiences of the engineer. Moreover, defining a new time varying boundary layer may also be suggested to overcome the chattering phenomenon.

APPENDIX A: Q-2-DOF-HS COMPONENTS

The components comprising the helicopter model are labeled in Figures A.1 [1], A.2 [1], A.3 [1] and A.4 [1] are described in the following table [1].

ID	Description	ID	Description
1	Back propeller	13	Metal shaft (rotates about yaw axis)
2	Back propeller shield	14	Slipring
3	Yaw/back motor	15	Yaw encoder
4	Pitch encoder	16	Base platform
5	Yoke	17	Front motor connector
6	Helicopter body	18	Right motor connector (not used)
7	Front propeller	19	Back motor connector
8	Pitch/front motor	20	Yaw encoder connector
9	Front propeller shield	21	Roll encoder connector (not used)
10	Encoder/motor circuit	22	Pitch encoder connector
11	Encoder connector on circuit (not used)	23	Left motor connector (not used)
12	Motor connector on circuit		

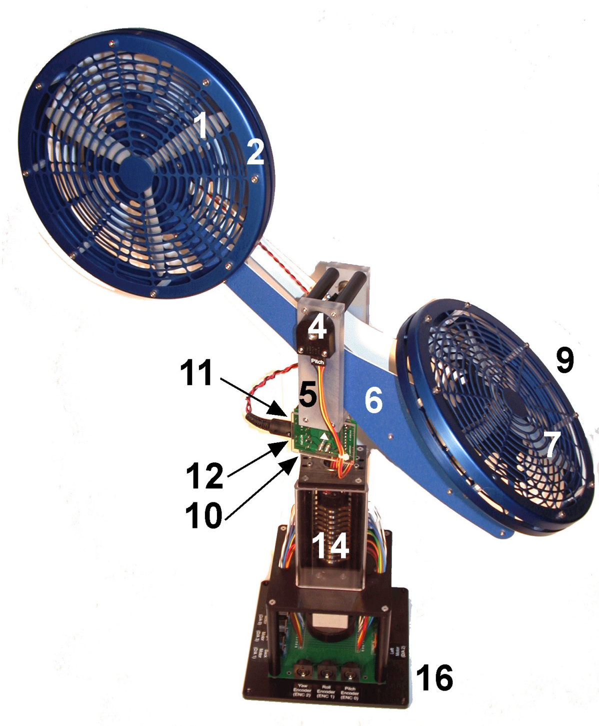

Figure A.1. Main components.

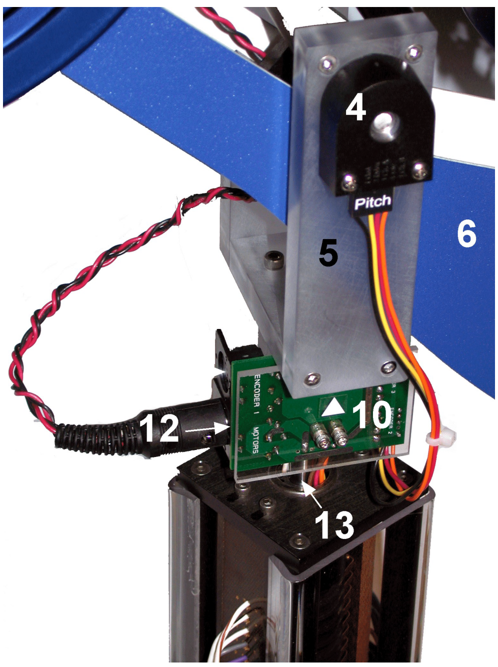

Figure A.2. Yoke components.

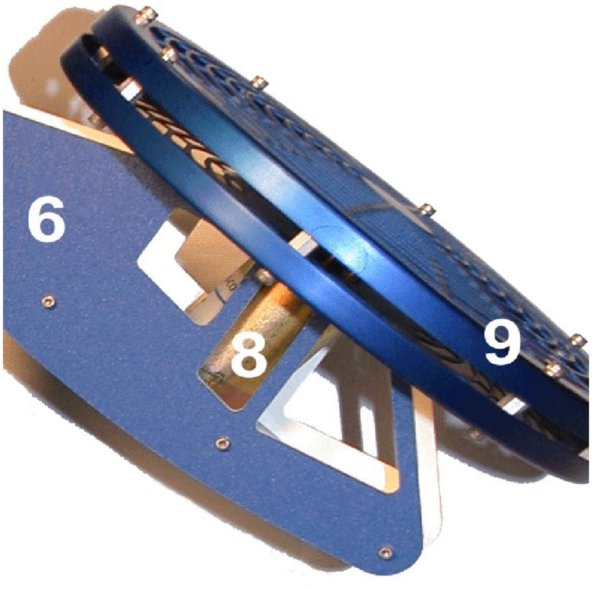

Figure A.3. Front components.

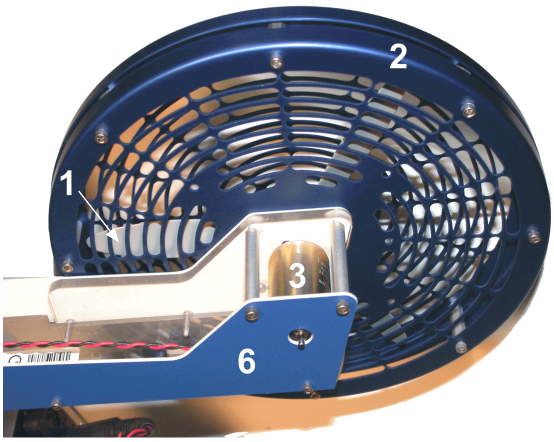

Figure A.4. Tail components.

While the pitch encoder is mounted directly to the shaft which is located above the center of the fuselage, the pitch encoder has slipring design. This special design eliminates the possibility of wires tangling of the wires and allows the helicopter to rotate fully around the yaw axis.

APPENDIX B: PARAMETERS IN MATHEMATICAL MODEL OF 2-DOF-HS

Constant Parameter	Value	Source
$K_{pp}\,(Nm/V)$	0.0515	Found experimentally
$K_{py}\,(Nm/V)$	0.015	Found experimentally
$K_{yy}\,(Nm/V)$	0.072	Found experimentally
$K_{yp}\,(Nm/V)$	0.037	Found experimentally
$J_p\,(kg\,m^2)$	0.0384	Given in the manual
$J_y\,(kg\,m^2)$	0.0432	Given in the manual
$B_p\,(N/V)$	0.04	Found experimentally
$B_y\,(N/V)$	0.55	Found experimentally
$m_{heli}\,(kg)$	1.3872	Given in the manual
$g\,(m/s^2)$	9.81	Given in the manual
$l_{cm}\,(m)$	0.0517	Theoretically derived

REFERENCES

1. *User Manual for 2-DOF Helicopter*, Revision 2.3 Quanser Consulting Inc.

2. Slotine, J. and W. Li, *Applied Nonlinear Control*, Vol. 199, Prentice-Hall Englewood Cliffs, New Jersey, 1991.

3. Dutka, A., A. Ordys and M. Grimble, "Non-linear Predictive Control of 2 DOF Helicopter Model", *Decision and Control, Proceedings. 42nd IEEE Conference on*, Vol. 4, pp. 3954–3959, IEEE, 2003.

4. Lopez-Martinez, M., J. Diaz, M. Ortega and F. Rubio, "Control of a Laboratory Helicopter Using Switched 2-Step Feedback Linearization", *American Control Conference, Proceedings*, Vol. 5, pp. 4330–4335, IEEE, 2004.

5. Ahmad, S., A. Chipperfield and O. Tokhi, "Dynamic Modeling and Optimal Control of a Twin Rotor MIMO system", *National Aerospace and Electronics Conference, Proceedings*, pp. 391–398, IEEE, 2000.

6. Yu, G. and S. Chen, "Nonlinear Flight Control of a Two-Degree-of-Freedom Helicopter Using Takagi-Sugeno Fuzzy Model", *Systems, Man and Cybernetics*, Vol. 5, pp. 4354–4359, IEEE, 2006.

7. Su, J., C. Liang and H. Chen, "Robust Control of a Class of Nonlinear Systems and Its Application to a Twin Rotor MIMO System", *Industrial Technology*, Vol. 2, pp. 1272–1277, IEEE, 2002.

8. Yu, G. and H. Liu, "Sliding Mode Control of a Two-Degree-of-Freedom Helicopter via Linear Quadratic Regulator", *Systems, Man and Cybernetics*, Vol. 4, pp. 3299–3304, IEEE, 2005.

9. Ahmed, Q., A. Bhatti, S. Iqbal and I. Kazmi, "2-Sliding Mode Based Robust Con-

trol for 2-DOF Helicopter", *Variable Structure Systems (VSS), 11th International Workshop on*, pp. 481–486, IEEE, 2010.

10. Baruh, H., *Analytical Dynamics*, WCB/McGraw-Hill, Boston, 1999.

11. Rahideh, A. and M. Shaheed, "Mathematical Dynamic Modelling of a Twin-Rotor Multiple Input-Multiple Output System", *Proceedings of the Institution of Mechanical Engineers, Part I: Journal of Systems and Control Engineering*, Vol. 221, No. 1, pp. 89–101, 2007.

12. *Dynamic Equations for the 2-DOF Helicopter*, Quanser Consulting Inc. 2006.

13. Franklin, G., J. Powell, A. Emami-Naeini and J. Powell, *Feedback Control of Dynamic Systems*, Vol. 2, Addison-Wesley Reading, New Jersey, 1994.

14. Richard, C. and H. Robert, "Modern Control Systems", *Prentice-Hall, Inc., New Jersey*, 2001.

15. Ogata, K., *Modern Control Engineering*, Prentice Hall, New Jersey, 2001.

16. *Laboratory Manual for 2-DOF Helicopter*, Revision 2.3 Quanser Consulting Inc.

17. Zanasi, R., C. Bianco and A. Tonielli, "Nonlinear Filters for the Generation of Smooth Trajectories", *Automatica*, Vol. 36, No. 3, pp. 439–448, 2000.